

CHAPTER 1

INTRODUCTION

1.1 Background of Study

Existing EOR methods in Oil and Gas Industry

During the past forty years, a variety of enhanced oil recovery (EOR) methods have been developed and applied mostly in depleted oil reservoir ^[1] in order to improve the efficiency of oil recovery compared with primary (pressure depletion) and secondary (water flooding) method. Using EOR, we can increase about 30% to 60% of the reservoir's original oil compared with 20% to 40% using the primary and secondary recovery.

EOR generally involves four methods, which are listed below ^[1];

1. **Thermal recovery** which is about the injection of hot steam to the second drilled hole. The steam will be used to heat the crude oil either during its flow upward in the drill head or in the pool, which would allow it to flow more easily toward the drill head. The introduction of heat such as the injection of steam is to lower the viscosity or thin the heavy viscous oil and improve its ability to flow through the reservoir.

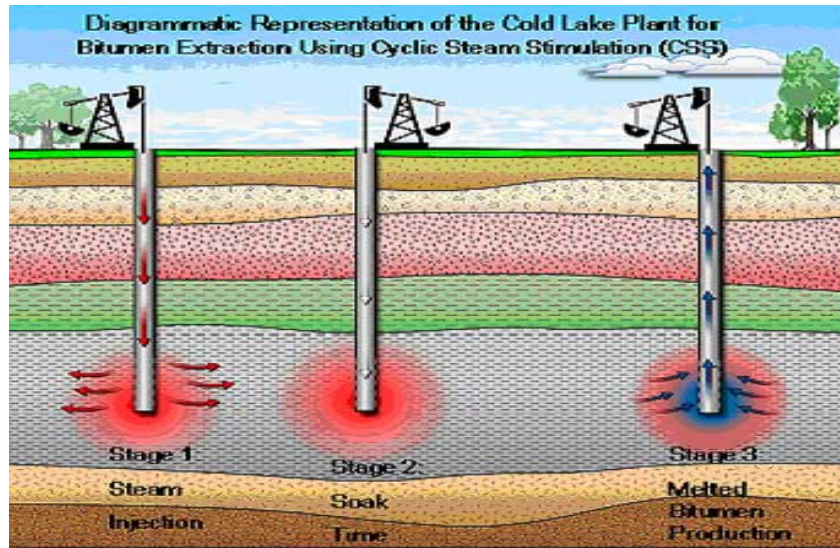


Figure 1: Thermal Recovery ^[2]

2. **Chemical injection** is applied by injecting the chemical substances like polymer into the reservoir to reduce the oil viscosity and increase the water viscosity.

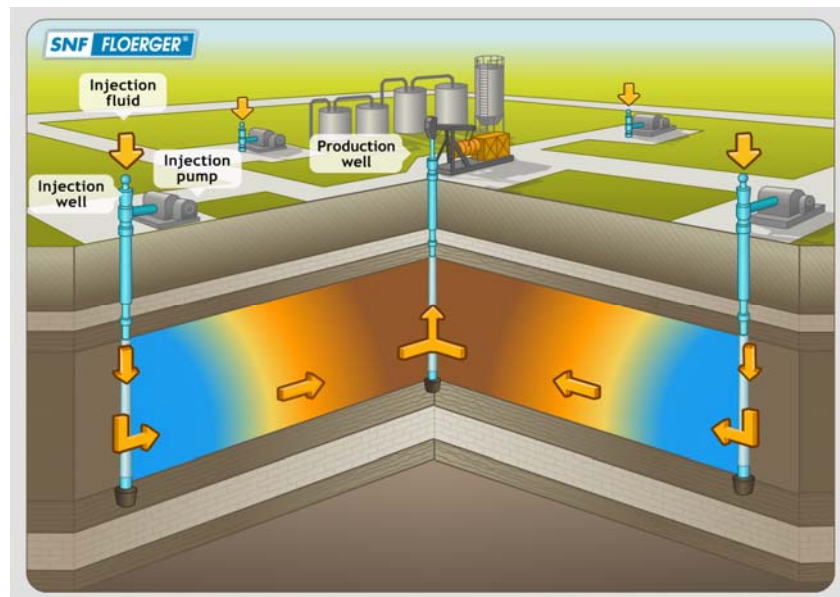


Figure 2: Chemical Injection ^[3]

3. **Gas injection** method is using the carbon dioxide gas, CO₂ or other natural gases like nitrogen where those gases are injected to the reservoir. The expansion of the CO₂ gas into the reservoir cause the oil is breaking up into droplet and easier to be pumped. Some of the natural gases used for injection purpose dissolve in the oil so as to lower the viscosity of the oil thus aiding in its enhanced extraction.

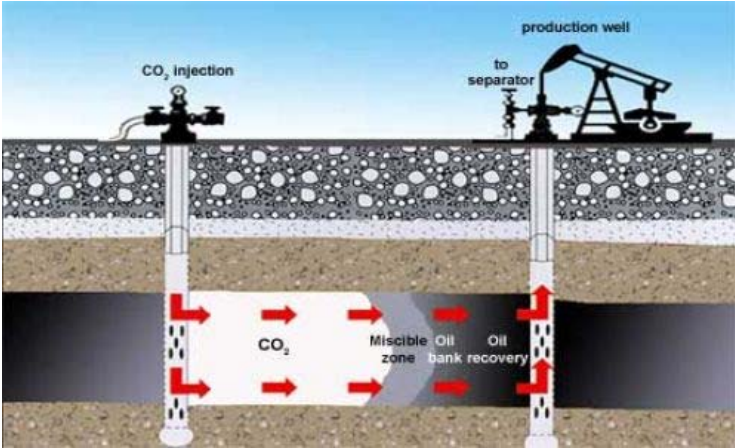


Figure 3: Gas Injection ^[2]

4. **Seismic approach** where by using this method, the oil trapped in the rock matrices is being 'vibrated' by the sound wave and then pumped up.

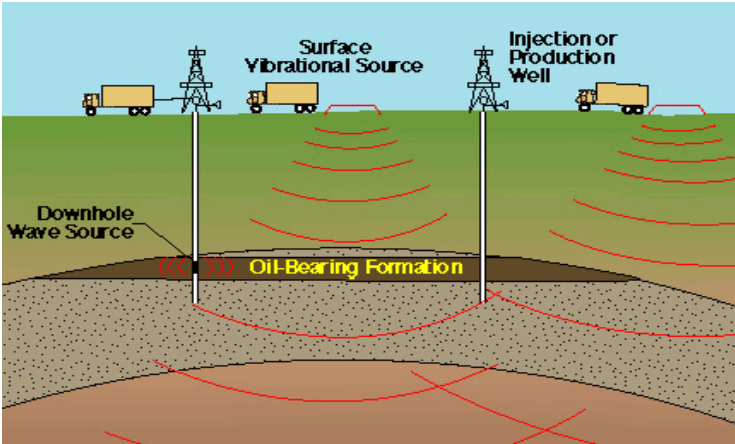


Figure 4: Seismic Approach ^[4]

Alternatively now, researcher found that EM waves have a big potential to be used as one of the EOR methods ^[5]. The characteristic of the EM waves that can penetrate deep through the reservoir itself be the main asset of why EM waves got the potential to be used inside the reservoir. Nowadays people use the EM waves to detect the hydrocarbon reservoir ^[6]. Hydrocarbon plays a very important role in dealing with the geometrical survey of the sub-surface structure.

This alternative method is used for the same objective, to maximize the crude oil production by at least with about 10% increment.

1.2 Problem Statement

Most wells produce complex, fractal drainage patterns that cause the oil to trap within the rocks. Low temperature and high pressure below 1000m cause the flow of fluid (oil) remain a challenge and this make the industrial to face a problem in improving the mobility of the heavy oil.

1.3 Objective and Scope of Study

1. To design and construct a transmitter that can transmit powerful EM waves to a core sample.
2. To evaluate the effect of electromagnetic waves diffusion to the crude oil mobility.
3. To calculate the oil recovery using EM method.

CHAPTER 2

LITERATURE REVIEW

2.1 Electromagnetic Waves

Maxwell equation stated that the magnetic field produced (B) is proportionally related to the current and the type of material used. The bigger current flow inside a conductor, and the higher the permeability of the material used, the bigger B field is produced ^[7].

Magnetic field (B) and the electric field (E) is propagating together perpendicularly with the same amplitude where the reduction in B field intensity will cause the same amount of reduction in E field as well ^[7].

Figure 5 shows how the E-field and B-field propagating perpendicularly in a medium and Figure 6 shows that the magnitude of E-field is proportional to the magnitude of B-field.

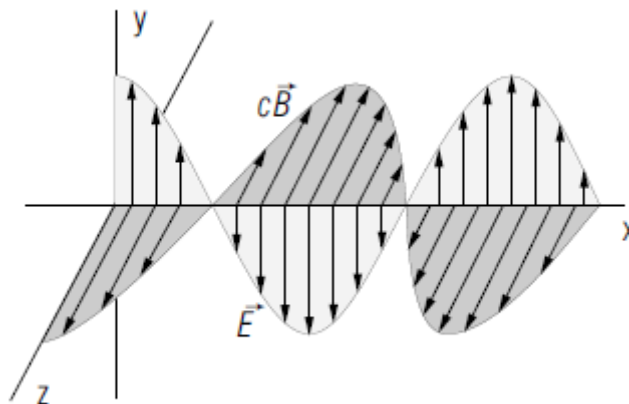


Figure 5: Electromagnetic Waves propagation ^[8]

Based on Maxwell equation ^[7],

$$B = \frac{\mu_0 I}{2\pi r}$$

where;

B = Magnetic field,

μ_0 = Magnetic Permeability

I = Current (A)

r = Distance

Overview by Peter Signell from Michigan State University, it is possible for E-field and B-field to propagate as waves in the empty space or we said as vacuum ^[9]. Electric and magnetic wave's field may exist in space without a material medium being present and if they vary in space and time in the appropriate way, the spatial variation will propagate as a wave, transporting energy. This module deals with the propagation of energy through a vacuum via electromagnetic disturbances whose space and time variation satisfy the conditions for wave propagation.

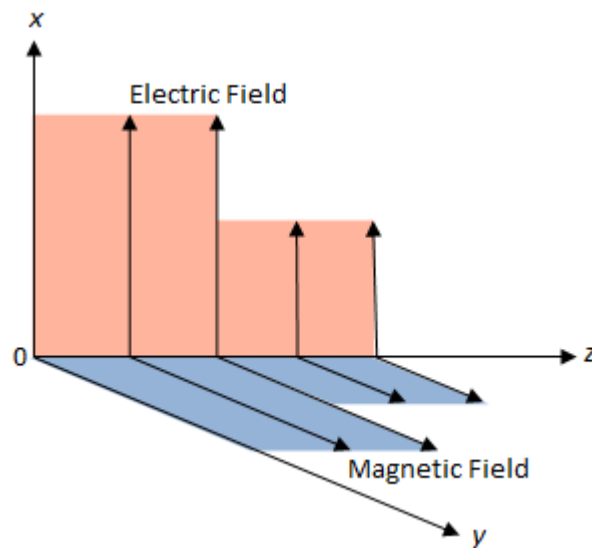


Figure 6: B field and E field propagation ^[10]

2.2 EM Transmitter and EM Detector

EM transmitter is defined as a radial waveguide that generates the EM wave while receiver is a radial waveguide that detects the EM wave ^[10]. Usually an EM transmitter uses turns of coil to generate the electromagnetic wave that is at a single frequency. When we apply a high frequency source of alternating voltage input to the coils/winding of the transmitter, a magnetizing current is developed in the winding itself. This magnetizing current then will generate an alternating flux in the magnetizable core that links the winding in order to develop an alternating polarity output voltage ^[11].

The amount of current induced depends on the electrical conductivity of the material itself ^[12]. Commonly we use copper as the transmitter since it is a highly electrically conductive material.

The currents induced in the transmitter then will generate a secondary EM field that can be detected using a receiver ^[12].

Commonly magnetic material like ferrite is used to construct the receiver. Magnetic material basically has the ability to gather or to concentrate the magnetic fields which then govern to the second induced currents ^[8].

The depth of penetration of the induced current can be calculated by using the skin depth equation. The smaller the skin depth will cause more induced current to concentrate at the skin of the magnetic material which will generate heat due to the eddy current.

Overviewed by Alex Becker, Ki Ha Lee and Lou Reginato from University of California on downhole EM transmitter using a 100m deep well at Richmond field station ^[13], EM transmitter was tested its performance toward the borehole to the surface configuration with a receiver and the result shown that EM transmitter specifically suited for subsurface use where the transmitted EM waves could be detected by the receiver. The designed EM transmitter was based on a long solenoid with a non-dissipative magnetic core. This finding shows that EM transmitter could be potentially applied to the reservoir which has fractional drainage pattern ^[13].

2.3 Radiation and Antennas

Shape and size of a transmitter determine how effective it is in extracting energy from the radio wave. Usually an antenna is designed so that it can radiate or receive electromagnetic energy with directional and polarization properties suitable for the intended purpose or application ^[7]. In order to design a transmitter, it is important to know the resistance of the antenna itself. The radiation and resistance properties of an antenna are governed by its shape and size and the material of which it is made.

The resistance and conductivity of an antenna has the relationship as follows ^[14];

$$R = \frac{\rho l}{A} \text{ And } \rho = \frac{1}{\alpha}$$

Where; R= Resistance

ρ = Resistivity

α = Conductivity

l = Length

A = Area

Radiation sources are classified into two groups; currents and aperture fields ^[7]. The dipole and loop antenna are examples of current sources while a horn antenna is one of the aperture source examples ^[7]. For current radiation source, the time- varying currents flowing in the conducting wires give rise to the radiated electromagnetic field ^[7]. In aperture source, the electric and magnetic fields across the horn's aperture serve as the sources of the radiated field. The aperture fields are themselves induced by time- varying currents on the surfaces of the horn's walls, and therefore ultimately all radiation is due to time- varying currents.

2.4 Skin Depth

The most important concept in any EM method is skin depth. EM energy decays exponentially in conductive rocks over a distance given by the skin depth ^[14]:

Skin depth = 500 meters x square root (resistivity/frequency).

In the seabed logging application, the skin depth equation $\delta = \sqrt{\frac{2}{\omega\mu\sigma}}$ is referred so that we could know how much EM waves would penetrate and diffuse into the reservoir ^[14], where σ is electrical conductivity, μ is magnetic permeability and ω is the angular frequency of the current.

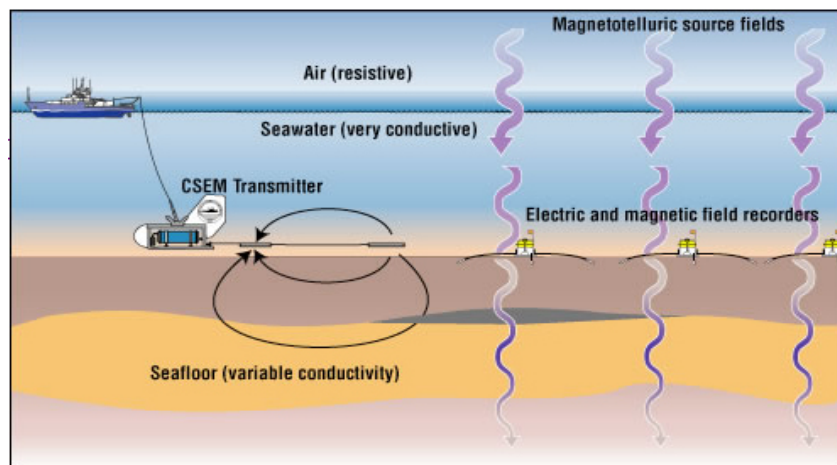


Figure 7: Field schematic for two electromagnetic techniques applied to offshore exploration--magneto telluric (MT) and marine controlled source electromagnetic (CSEM) sounding ^[15].

CHAPTER 3

METHODOLOGY

3.1 Tools and Equipments required

HARDWARE:

- I. Transmitters with magnetic feeders
- II. Receiver
- III. Function generator 5MHz and 80MHz
- IV. Tank 1.92m x 0.91m x 0.61m
- V. Core rock sample
- VI. Data acquisition system (DAS) Model NI PXI-1042 (for EM data storage)
- VII. DC power supply
- VIII. Weighing Apparatus
- IX. Temperature Controller
- X. DC Power Supply
- XI. Helium Porosimeter
- XII. Core Flooding Machine
- XIII. Caliper

SOFTWARE:

- I. CST (Computer Simulation Technology)
- II. Microsoft Office VISIO

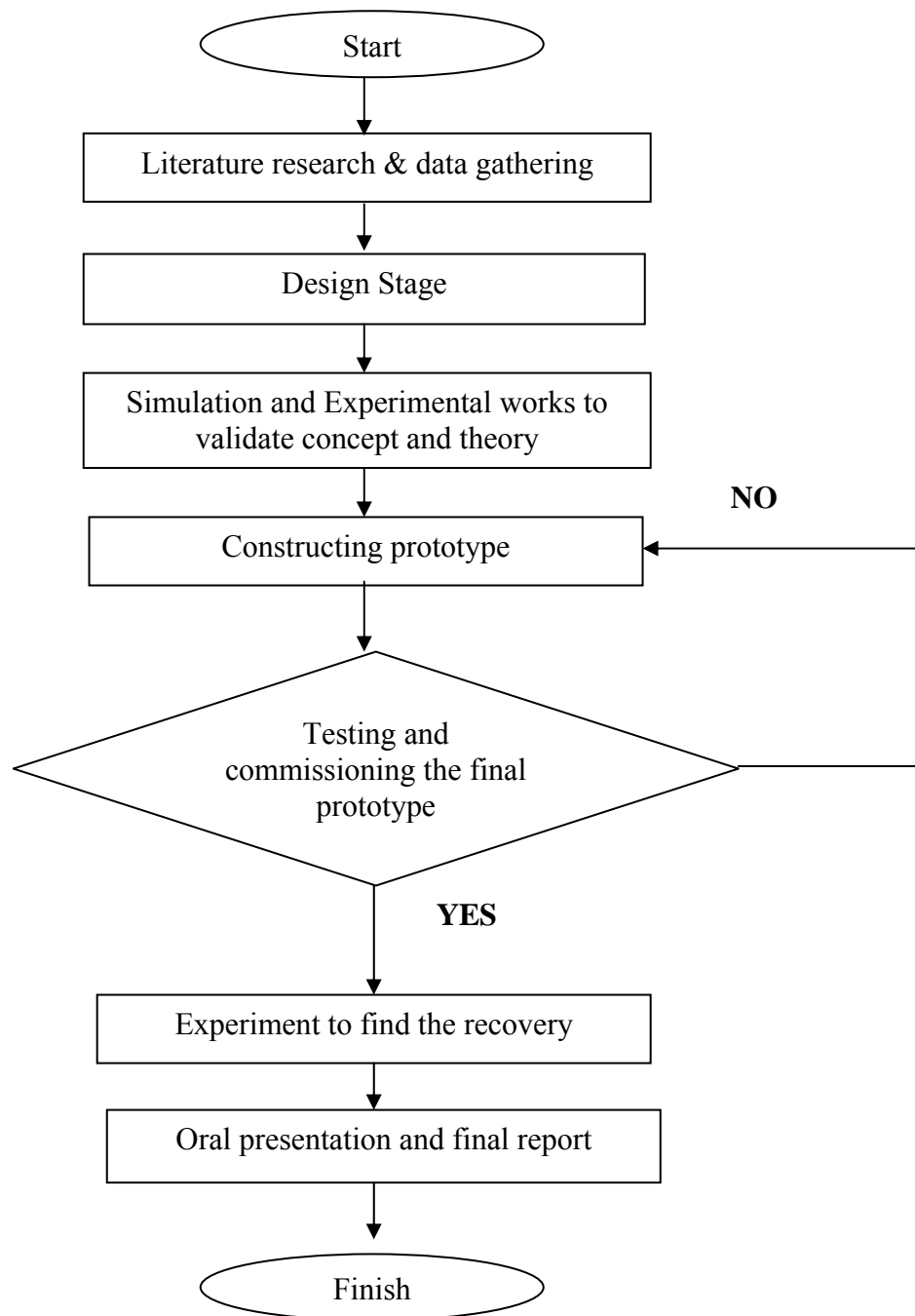


Figure 8: Project Process Flow Chart

3.2 Data Gathering

Based on the background study and the literature review, EM wave can be considered as a potential recovery method in the viscous oil reservoirs. In previous methods like ohmic heating, induction heating and formation resistive heating, current is injected in order to get the heat from the induction process. For the purpose of this project, the behavior of EM wave itself is being manipulated in order to increase the oil mobility where a powerful transmitter will be used to get the powerful EM waves.

Electromagnetic waves are created by the vibration of an electric charge. This vibration creates a wave which has both an electric and a magnetic component. An electromagnetic wave transports its energy through a vacuum at a speed of 3.00×10^8 m/s (a speed value commonly represented by the symbol c) [14]. By having certain kind of transmitter design, we could have a transmitter that can transmit more EM wave which can provide better electric charge vibration which can help to improve the oil mobility that trapped inside the reservoir.

Based on the previous research done by Nur Azliza Ahmad from Universiti Teknologi PETRONAS on Development of a Powerful EM Transmitter [16], it is showing that hexagon shape is best design for a transmitter. The design that has been made was using one source and the copper winding made was in straight pattern as shown in Figure 9;

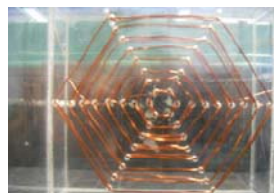


Figure 9: Hexagon transmitter with straight copper winding

3.3 Design Stage and Prototype Construction

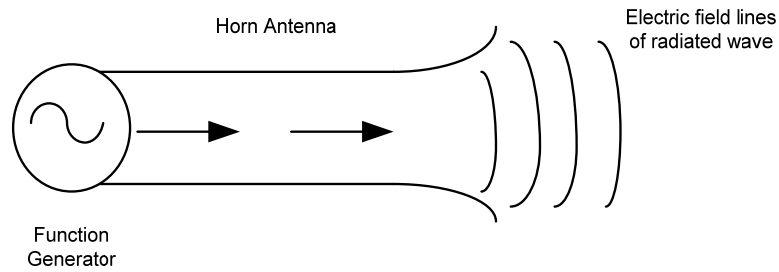


Figure 10: How a wave launched by a Horn Transmitter^[8]

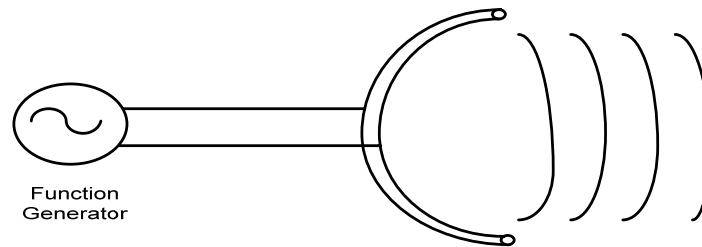


Figure 11: How a wave launched by a Curve Transmitter^[8]

In this project, the transmitter was designed based on the horn shape. Referring on the literature review, it stated that the horn shape is classified as the aperture field radiation sources where both electric and magnetic fields across the horn's aperture serve as the source of the radiated field which means, higher EM waves propagation produced.

The transmitter was also designed to be in hexagon shape with curve copper windings (6m) and has six supply sources (shown in Figure 14) compare to the previous design (Figure 9) which has straight copper windings and has only one supply source. The purpose of having the 6 curves winding shape is as it can provide a sharp and focus EM field. The winding wires was made from the copper since it is

a highly conductive material which then will governs to the bigger amount of induced current. Six supplies were connected to each 1m (six segments) of copper winding to create the constructive interference and this allows a higher EM waves transmission.

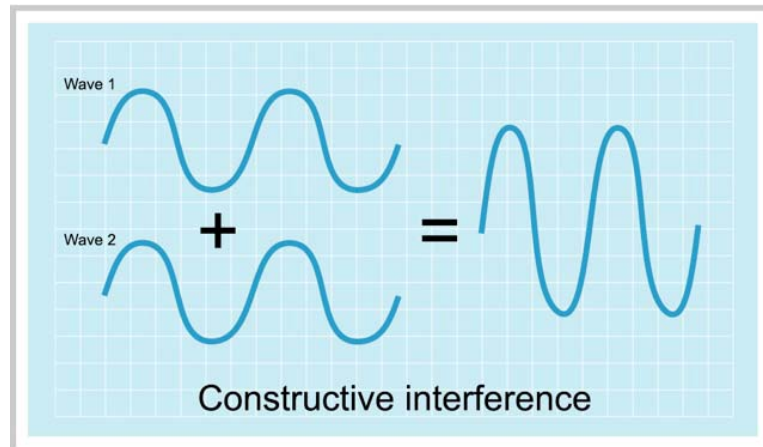


Figure 12: The Constructive Interference^[17]

Whenever the EM field travelling along the rocks (where there are oil trapped) it will carry along the energy and this cause the oils trapped are going to vibrate and thus will help them to release from the rock and become as the droplets. The skin depth theory is referred in order to know how much EM waves could penetrate and diffuse into the reservoir (see Figure 13).



Figure 13: Reservoir rocks have oil trapped in its pores

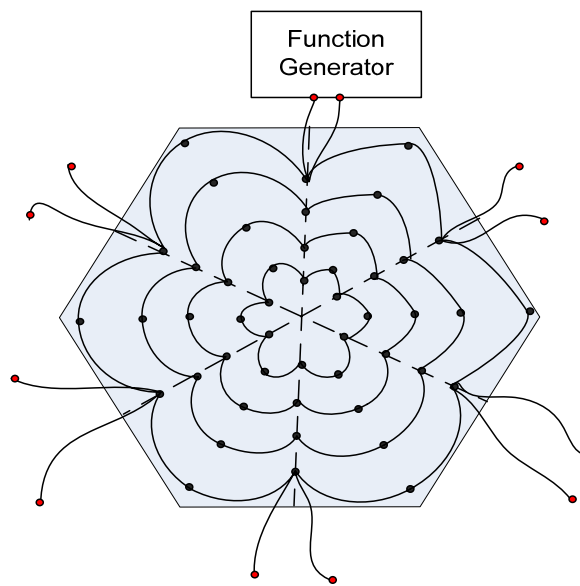


Figure 14: The Designed EM Transmitter which has six segments with 1m copper winding each. Each segment is connected to the 1 KHz frequency supply.

3.4 Experiment To Find The Recovery

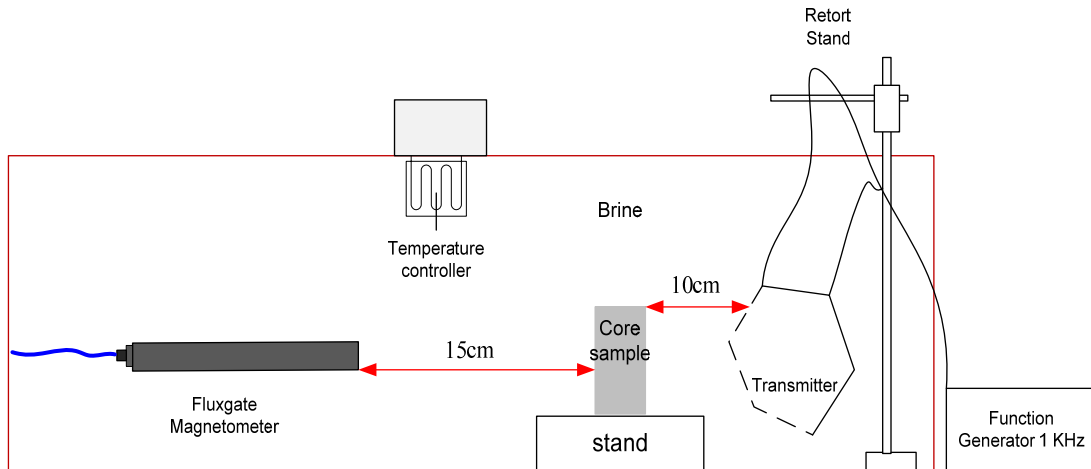


Figure 15: Schematic Diagram of the Experimental Setup

3.4.1 Tank

A tank with size of 1.92m X 0.91m X 0.61m was used with the temperature controller together.

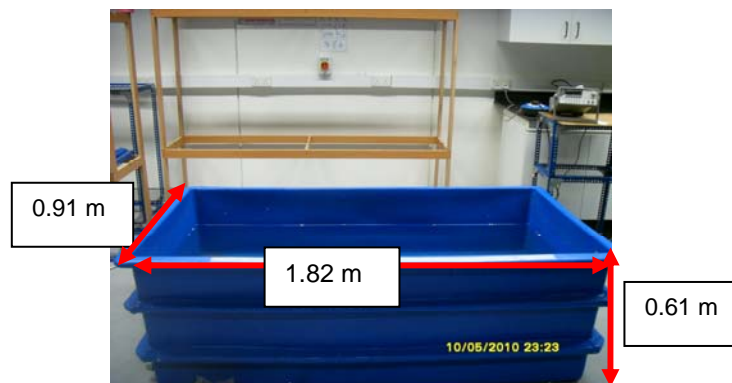


Figure 16: Tank

3.42 Transmitters

The transmitter was fabricated using the copper-curve shape wires in a hexagon-shape prospect. Power amplifier and magnetic feeders were used in order to increase the EM waves transmitted. This transmitter was constructed with six segments from 6m of copper wire winding and with 6 sources.

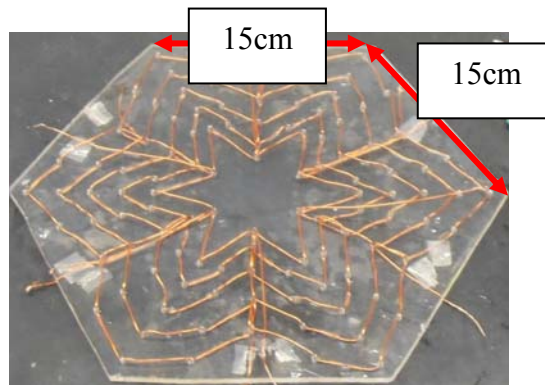


Figure 17: The designed EM Transmitter

3.43 Brine

Brine (density is 1.0061g/cm^3) water was used in order to conduct and allow the transmission of EM wave to the core rock.

3.44 Data acquisition system (DAS) Model NI PXI-1042 (for EM data storage) and Fluxgate Magnetometer Model Bartington.

DAS and Fluxgate Magnetometer were used in order to detect and store the data of the EM waves that transmitted through the core rock.

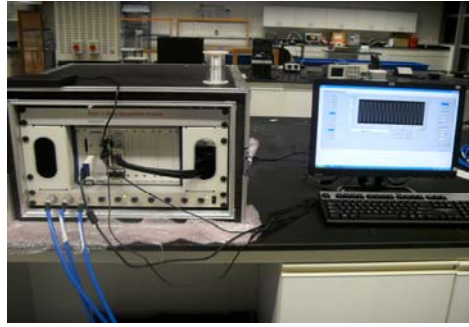


Figure 18: Data acquisition system (DAS) is a product and/or processes used to collect information to document or analyze some phenomenon.

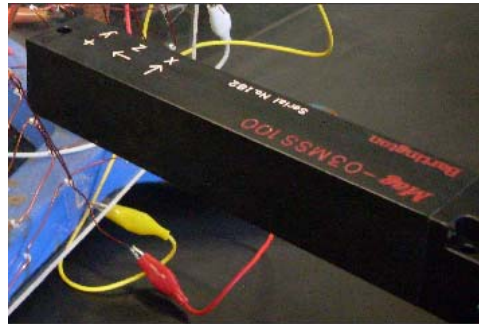


Figure 19: Fluxgate Magnetometer is capable of measuring the strength of any component of the Earth's magnetic field by simply re-orienting the instrument so that the cores are parallel to the desired component.

3.45 Temperature Controller

The temperature controller Protech SDC10 was used to maintain the temperature in order to get a reservoir-look-alike set up. The temperature in the tank for the experiments purpose is about 37°C.

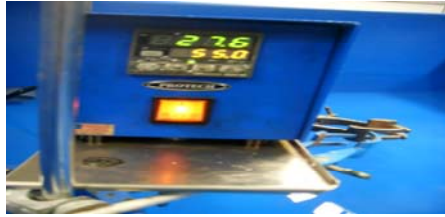


Figure 20: Protech SDC10 Temperature Controller is used to maintain the temperature of 0.91m x 1.82m x 0.61m tank to be around 37 °C

3.46 Function Generator

The 1 KHz function generator was used as the transmitter supply source and also as the supply to the magnetic feeder.



Figure 21: Function generator 5MHz model Instek GFG-8250A

3.47 DC Power Supply Model GPC-3030DQ

Dc power supply was used to supply the amplifier with 12V.



Figure 22: DC power supply

3.48 Amplifier

Power amplifier was used to increase or amplifies the amplitude of the signal which in this case, the current that flowing in the transmitter conductor. Higher current will contribute to higher EM wave's transmission. This amplifier is operated by supplying 12V DC supply and 1 KHz frequency.



Figure 23: Power Amplifier

3.49 Magnetic Feeder

Magnetic Feeder was used to increase amplitude of EM waves transmitted by the designed transmitter.

These feeders were prepared using sol gel method which resulted in getting nanoparticles. The nanoparticles were formed to toroid shaped sample with 0.5cm outer diameter and 0.25cm in height (refer to Table 1).



Figure 24: Nanoparticle Magnetic Feeder

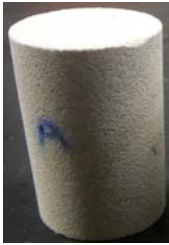
Table 1: Magnetic feeder characteristics

Parameter	700° C	900° C
Weight (g)	0.5	0.5
Outer Diameter (cm)	0.5	0.5
Inner Diameter (cm)	0.25	0.25
Height (cm)	0.25	0.25
Density (g/cm³)	3.4	3.4
Number of winding	20	20
Material of winding	Copper wire	Copper wire

3.50 Core Rock samples

The core rock sample used has the below characteristics:

Table 2: Core Sample Characteristics

<p>Core rock with sample ID: A</p>  <p>Figure 25: The Core Sample</p>	<p>Length(mm): 73.66</p> <p>Weight(g): 171.53</p> <p>Diameter(mm): 38.02</p> <p>Permeability: 567.8002</p> <p>V_p(cc), Pore Volume: 17.7657</p> <p>Φ(%), Porosity: 21.1771</p> <p>V_{grain} (g/cc): 66.1254</p> <p>V_{bulk}(g/cc): 83.8910</p>
--	--

3.51 Helium Porosimeter

Helium Porosimeter was used in order to analyze the main data measurements for the core sample which are the pore volume, porosity and permeability. Porosity is the percentage that the volume of the pore space bears to the total bulk volume, which is the pore space that determines the amount of space available for storage of fluids.

Pore volume is the volume of connected pores in a core sample in which the fluids can flow, and permeability is the ability of a rock to transmit fluid through the pore spaces.



Figure 26: Helium Porosimeter

3.52 Core Flooding Machine

Core flooding machine was used in order to prepare the core sample with the brine and also with the crude oil. For this purpose, a syringe pump introduces a fluid into the core holder (see Figure 28). The process of the flooding was involved with the used of injection of brine and crude oil at a high pressure

and low flow rates. For the data obtained from the core rock flooding, we can device the EM wave method to recover as much oil as possible.

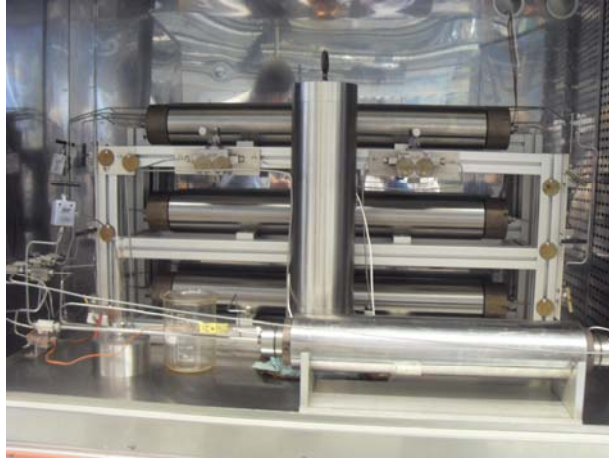


Figure 27: The Core Flooding Machine

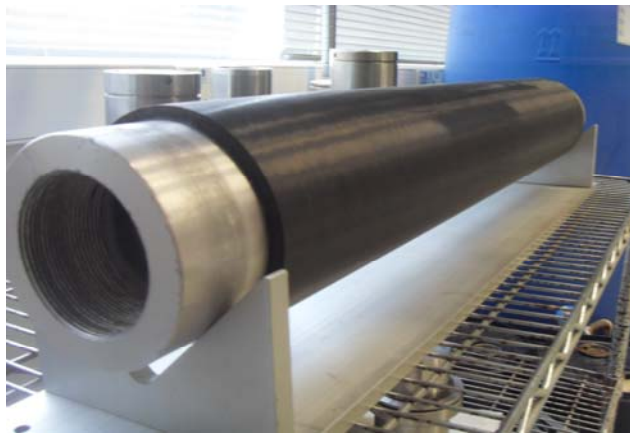


Figure 28: The Core Holder

3.53 Weighing Apparatus

The weighing apparatus was used to weight the core sample from time to time. The weighing apparatus with three decimal places was used in order to get more accurate measurements which are very important in the recovery calculation.

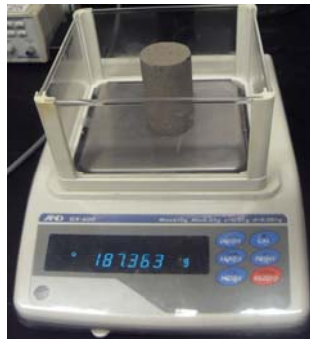


Figure 29: Weighing Apparatus

3.54 Caliper

Caliper was used to measure the height, wide and thickness of the core sample. These measurements are then used to the Helium Porosimeter in order to check their porosity, pore volume and permeability.



Figure 30: Caliper

3.55 CST (Computer Simulation Technology) software

The electromagnetic simulation software CST STUDIO SUITE™ is the culmination of many years of research and development into the most efficient and accurate computational solutions to electromagnetic design. It comprises CST's tools for the design and optimization of devices operating in a wide range of frequencies – static to optical. Analyses may include thermal and mechanical effects, as well as circuit simulation. All programs are accessible through a common interface with facilitates circuit and multi-physics co-simulation.

By using CST, the significant of transmitter's shape can be analyzed based on the E-field and B-field produced.

CHAPTER 4

RESULTS AND DISCUSSION

Experiment 1: Simulation on Straight and Curve wire

Equipments and materials used: CST (Computer Simulation Technology)

Description:

This simulation was done in order to see how the E-field and B-field transmitted pattern in straight and curve wire is looked like and thus to determine which pattern is the best in term of E-field and B-field to be the transmitter base. Straight aluminium wire (15.7cm long) and curve aluminium wire (15.7cm long and 10cm in diameter) were used. Both wire pattern were supplied with 1 KHz frequency and injected with 20 A of current.

Results:

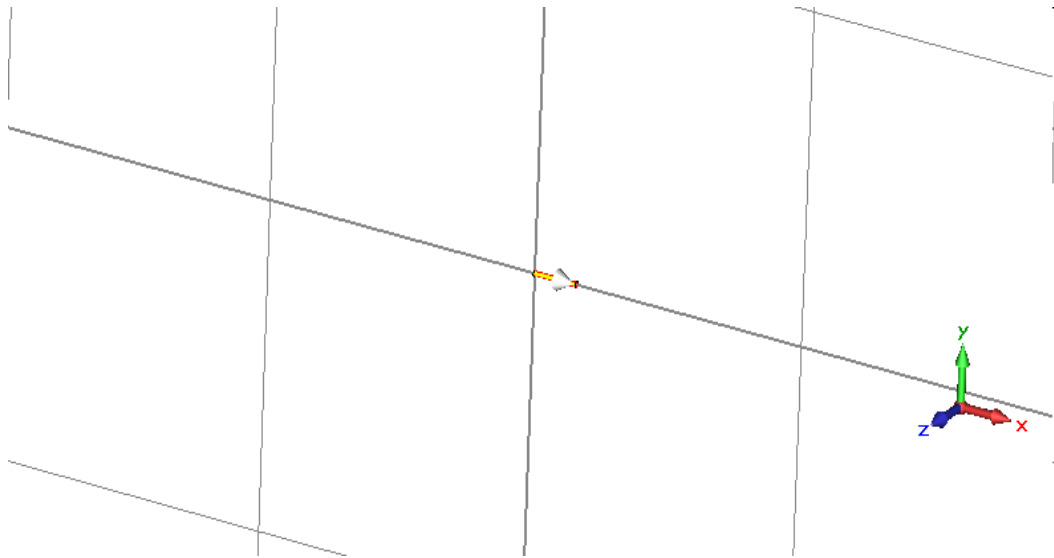


Figure 31: Current path in a 15.7cm straight Wire

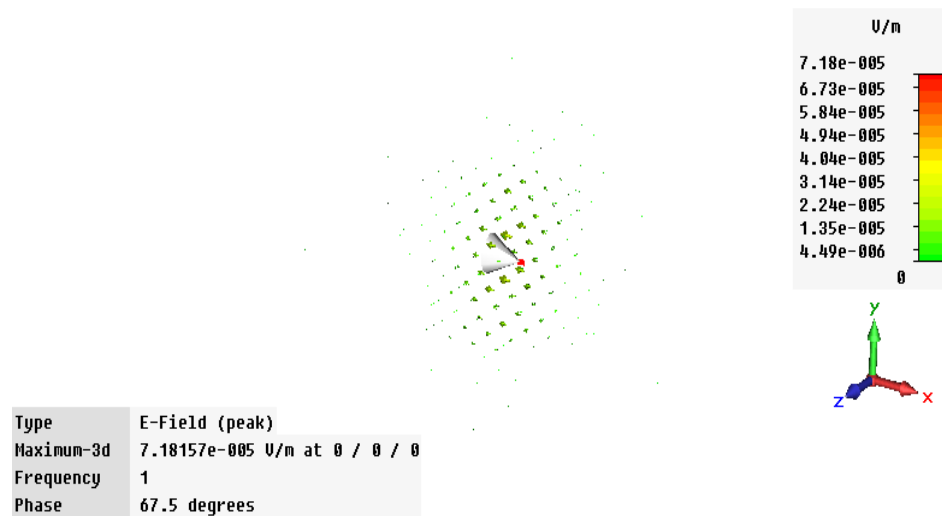


Figure 32: The electric field produced in Straight Wire
(Maximum is $7.81e^{-005}$ Vs/m²)

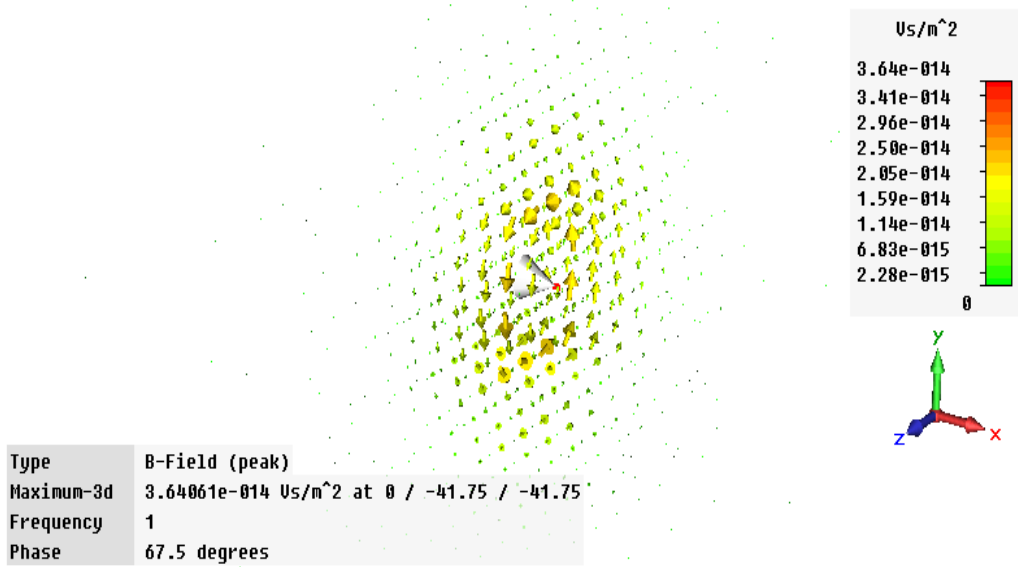


Figure 33: The magnetic field produced in Straight Wire
(Maximum is $3.64e^{-14}$ Vs/m²)

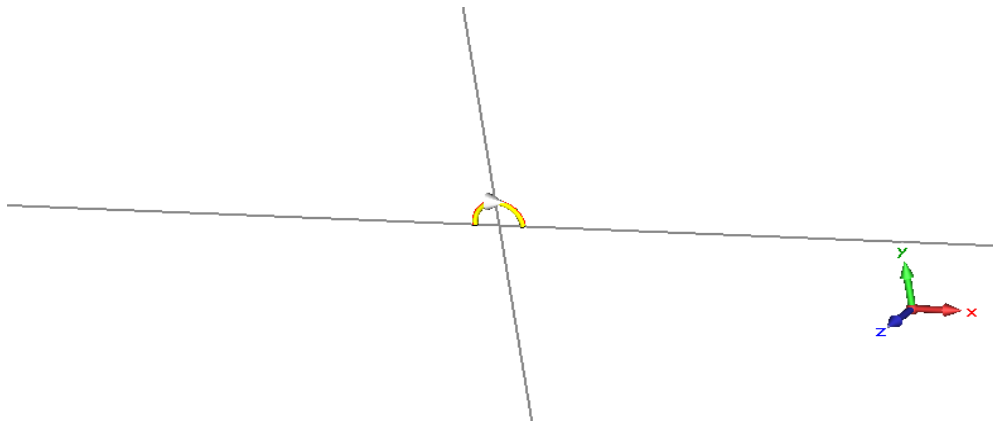


Figure 34: Current Path in Curve Wire

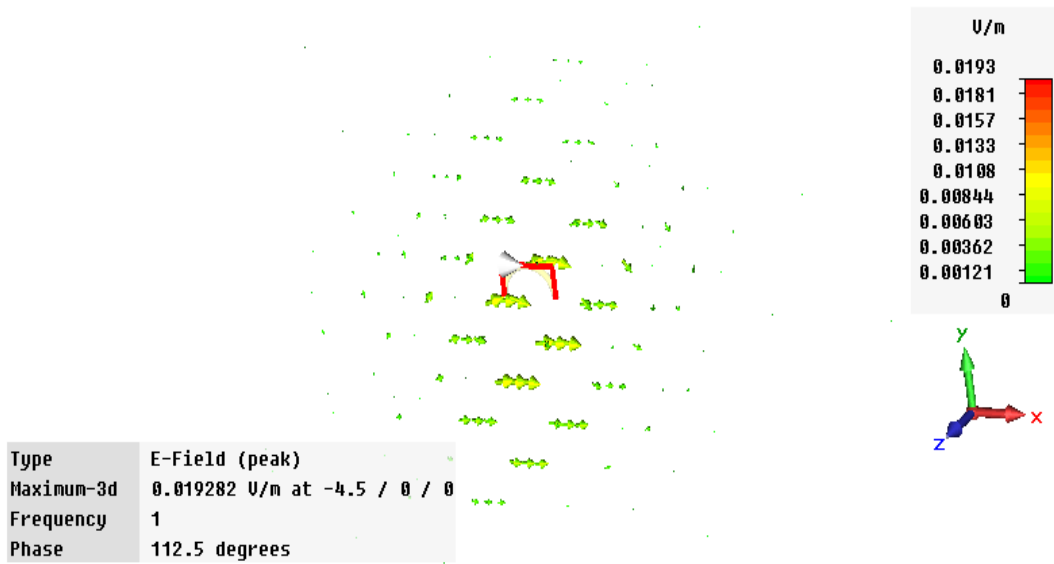


Figure 35: The electric field produced in Curve Wire
(Maximum is 0.0193 V/m)

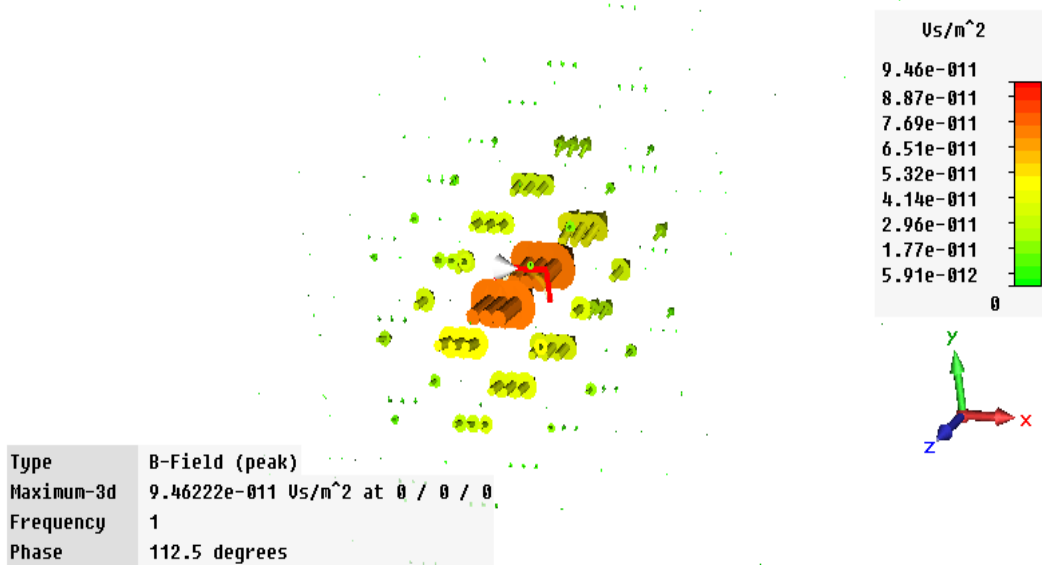


Figure 36: The magnetic field produced in Curve Wire
(Maximum is 9.46×10^{-11} Vs/m²)

Discussion and Conclusion:

From the simulation results shown, we could see that there are different patterns of how E-field and B-field distribution are. With curve aluminum wire, the B-field distribution is likely more focused rather than B-field in straight wire which is equally distributed. The characteristic of focused B-field with higher value compared to the straight wire is very important in order to design a good EM transmitter.

The electric field produced is higher in a curve wire compare to the straight wire with 99.6% of increment. Table 3 shows that the value of both B-field and E-field in curve wire is higher than in straight wire.

Table 3: B field and E field

	Curve Wire	Straight Wire
B field (T)	$9.46e^{-11}$	$3.64e^{-14}$
E field(V/m)	0.0193	$7.81e^{-5}$

Experiment 2: Designing EM Transmitter Using CST

Equipments and materials used: CST (Computer Simulation Technology)

Description:

This simulation was done in order to see the significant of having more aluminum wires instead of having just one wire as the transmitter base. The primary simulation was carried out by considering the straight aluminum wire instead of curve wire and to be understood that the results for curve wires would be exceeding base on the results in experiment 1.

The simulation was made with a 15cm straight aluminum wire. For this experiment, 80 MHz and 20A of current were supplied to the model. The aluminum wire numbers then were increased up to eight and the B-field distributions were recorded and analyzed.

Results:

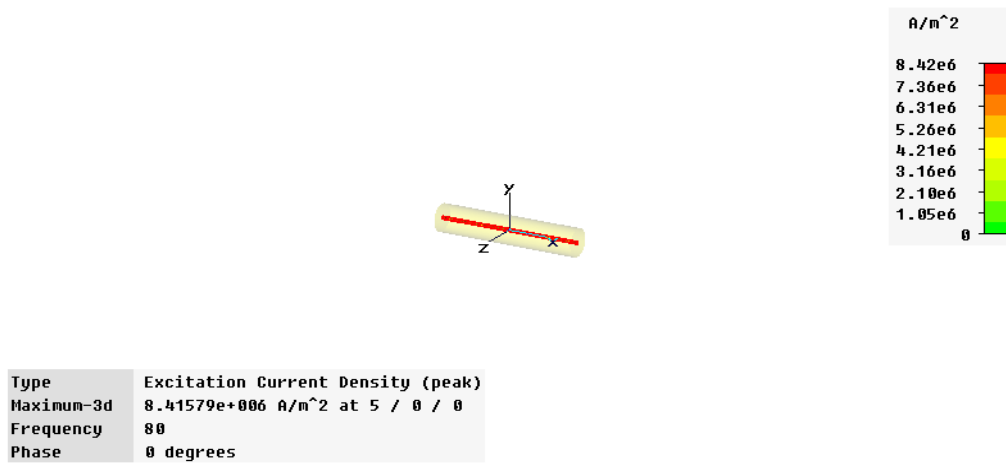


Figure 37: Source Current in one straight wire

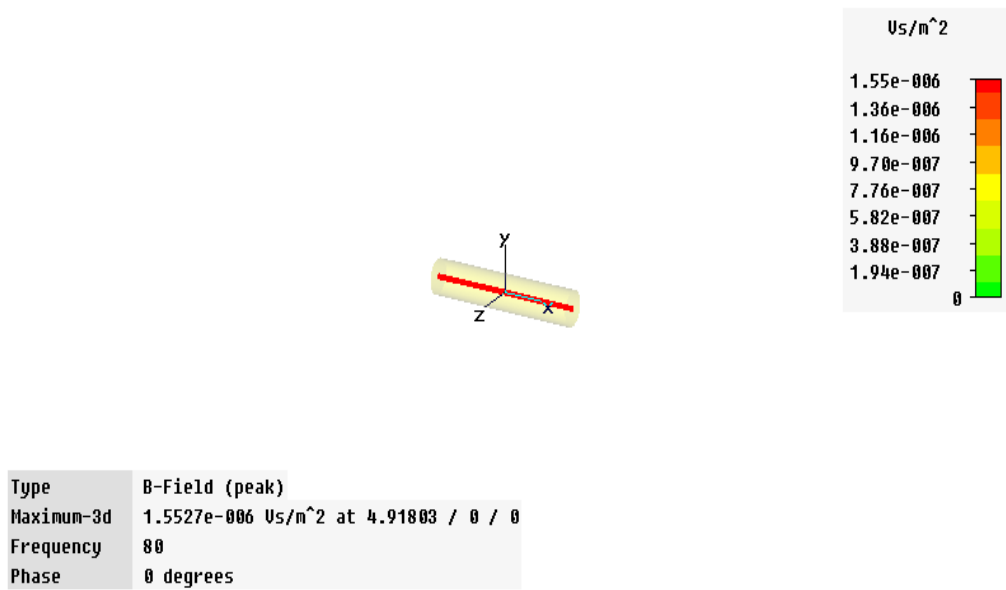


Figure 38: B-field distribution in one straight wire

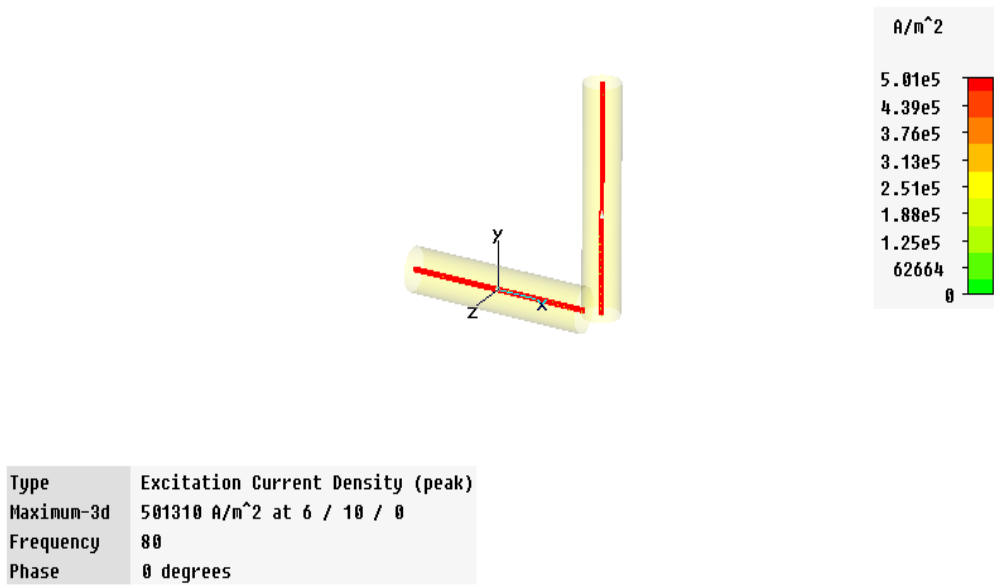


Figure 39: Source Current in two straight wires

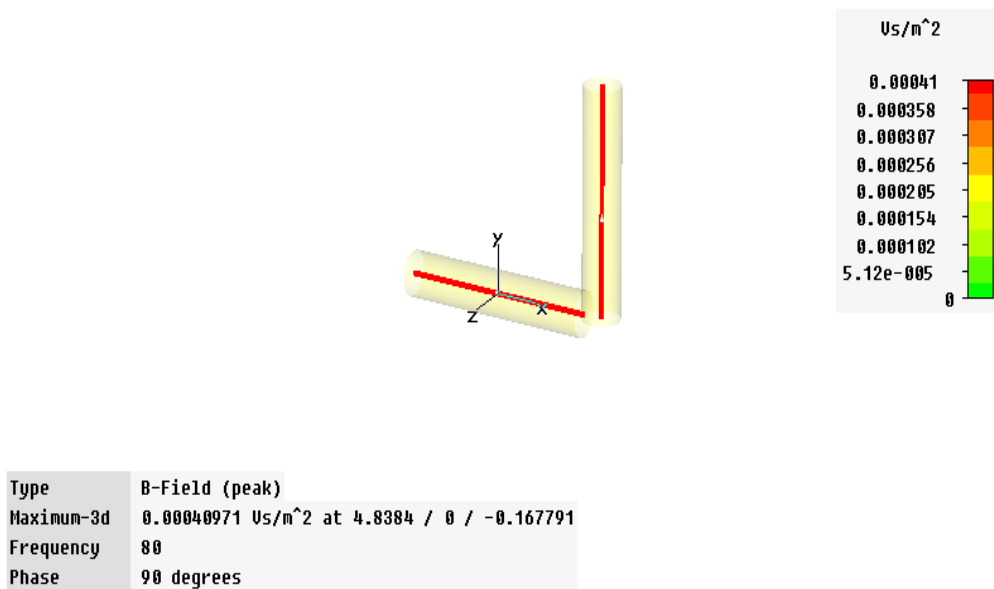


Figure 40: B-field distribution in two straight wires

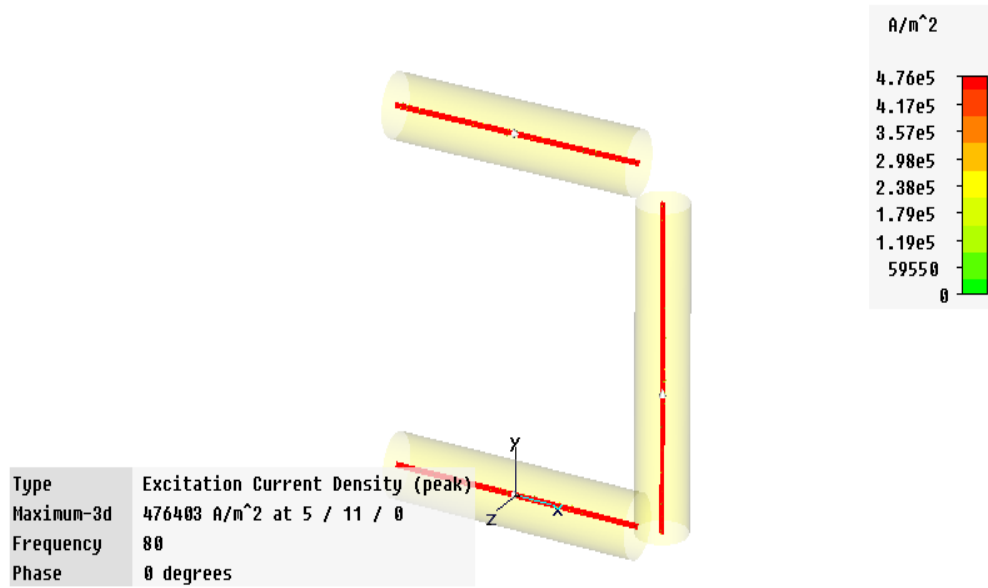


Figure 41: Source Current in three straight wires

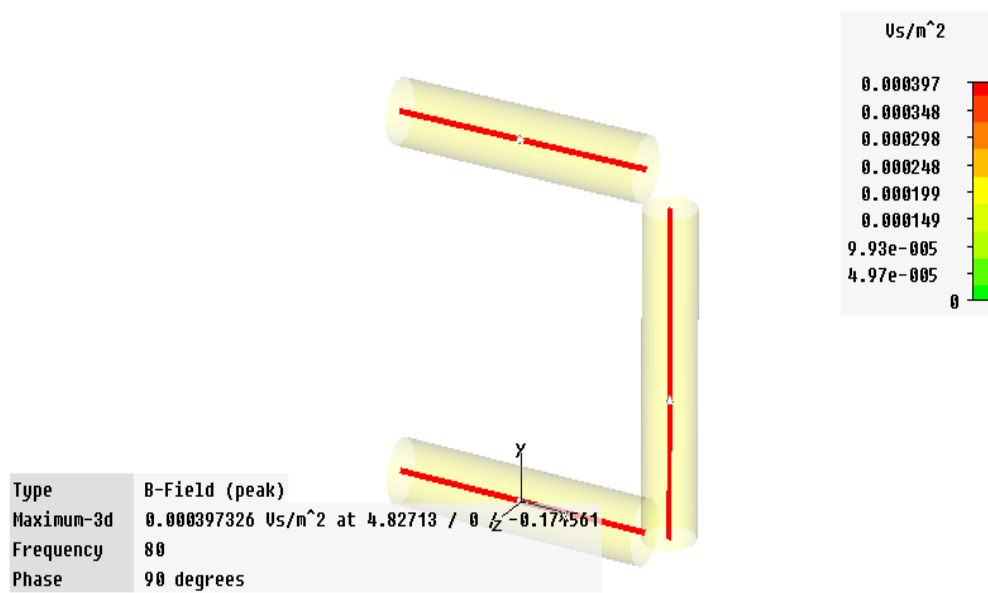


Figure 42: B-field distribution in three straight wires

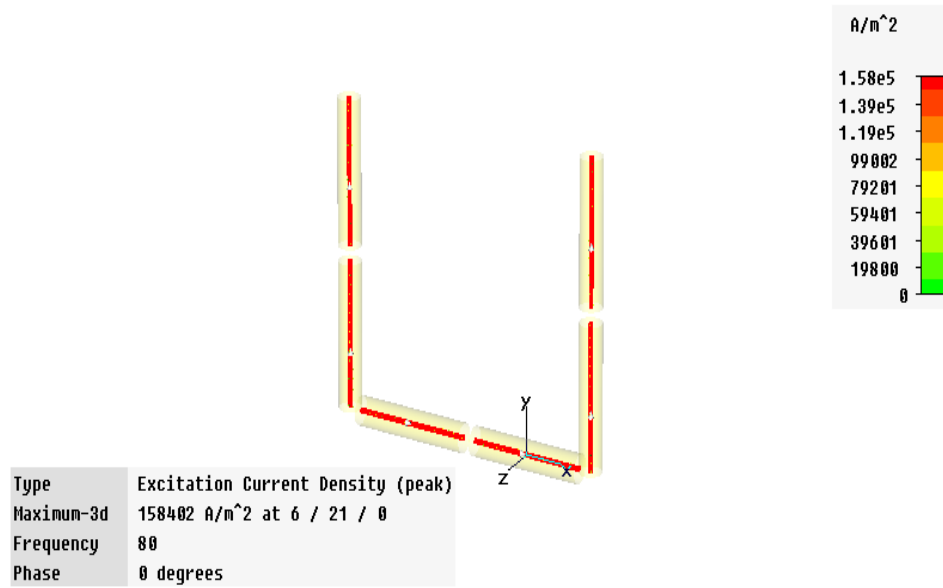


Figure 43: Source Current in six straight wires

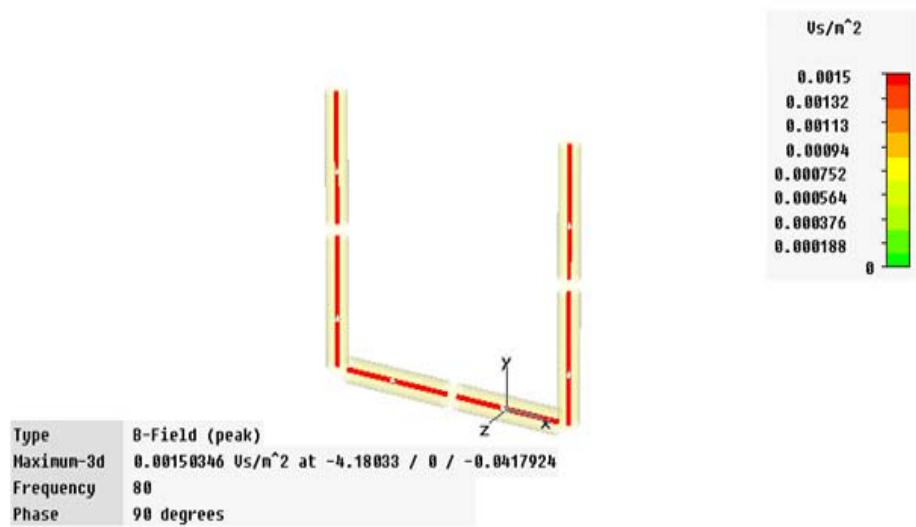


Figure 44: B-field distribution in six straight wires

Discussion and Conclusion:

Referring to the results of simulation done, the significant of having more aluminum wires are shown up to eight aluminum wires used where the B-field distribution is increasing proportional to the increment of the aluminum wires. However, the significant of having more wires are not applicable to the number of wire more than six where the value of B-field distribution is start to decrease.

The six straight wires give the highest value of magnetic field distribution which is 0.0015T.

Table 4 shows the data on B-field distribution for the numbers of aluminum wires used in this simulation.

Table 4: The distribution of B-field in one up to eight wires

Number of straight wire	B-field (T)
1 wire	0.00000155
2 wires	0.00041
3 wires	0.000397
4 wires	0.000520
5 wires	0.000632
6 wires	0.0015
7 wires	0.000861
8 wires	0.000797

Experiment 3: Experimental Work on the Significant of Supply Connection

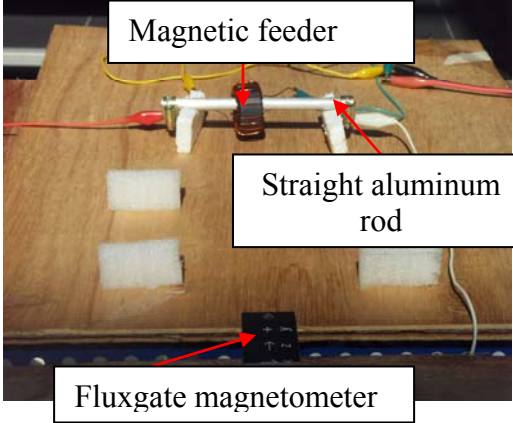
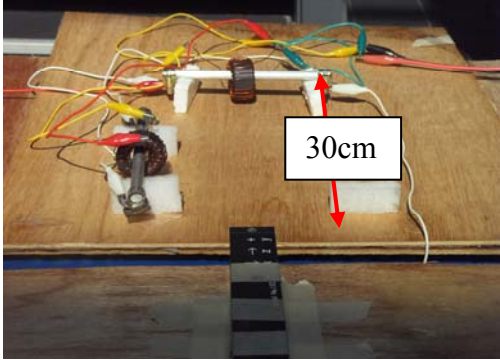
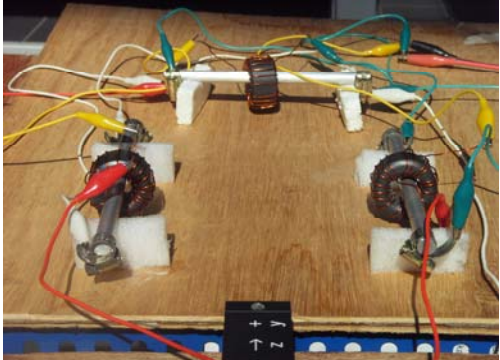
Equipments and materials used:

1. Function generator 5MHz
2. Straight aluminium rods (transmitter) with length of 15.7cm
3. Magnetic feeder with frequency supply equal to 1Khz
4. Fluxgate magnetometer
5. Wire clippers

Description:

The purpose of this experiment done was to investigate the significant of having different type of supply connections which are series connection or parallel connection when having more than one wire in one time. Due to the availability of materials in lab, the experiment conducted was on the three straight aluminium rods with 15cm long and 1cm in diameter. In the first run, one straight rod with magnetic feeder was connected to the 5 MHz function generator and both were supplied with 1 KHz frequency. The rod with the magnetic feeder then left for about half an hour with the fluxgate magnetometer in order to get better and accurate data of B-field distribution by the straight rod aluminium. The fluxgate magnetometer was placed 30cm apart from the aluminium rod.

The experiment was furthered by considering two and three aluminium rods with magnetic feeder by applying both type of supply connections, series and parallel. The B-field distribution produced by the aluminium rods then has been identified by the fluxgate magnetometer.

 <p>Figure 45</p>	<p>1 Straight rod</p>
 <p>Figure 46</p>	<p>2 Straight rods with parallel supply connection</p>
 <p>Figure 47</p>	<p>3 Straight rods with parallel supply connection</p>

Results:

Table 5: The average of magnetic field produced by 1 straight rod with a power source

1 rod_1	1 rod_2	1 rod_3	Ave
4.18E-08	4.13E-08	4.21E-08	4.17E-08
4.29E-08	4.20E-08	4.17E-08	4.22E-08
4.27E-08	4.25E-08	4.23E-08	4.25E-08
4.20E-08	4.17E-08	4.19E-08	4.19E-08
4.22E-08	4.23E-08	4.16E-08	4.20E-08
4.24E-08	4.22E-08	4.19E-08	4.22E-08
4.19E-08	4.17E-08	4.15E-08	4.17E-08
4.24E-08	4.22E-08	4.22E-08	4.23E-08
4.25E-08	4.22E-08	4.23E-08	4.23E-08
4.25E-08	4.24E-08	4.22E-08	4.24E-08
4.20E-08	4.17E-08	4.21E-08	4.19E-08
4.23E-08	4.24E-08	4.21E-08	4.23E-08
4.28E-08	4.19E-08	4.21E-08	4.23E-08
4.22E-08	4.25E-08	4.22E-08	4.23E-08
4.17E-08	4.27E-08	4.18E-08	4.21E-08
			4.21E-08

Table 6: The average of magnetic field produced by 2 straight rods with parallel power source

2 rods_dif source_1	2 rods_dif source_2	2rods_dif source_3	Ave
9.48E-07	9.59E-07	9.29E-07	9.45E-07
9.48E-07	9.57E-07	9.30E-07	9.45E-07
9.48E-07	9.55E-07	9.29E-07	9.44E-07
9.49E-07	9.57E-07	9.28E-07	9.45E-07
9.46E-07	9.59E-07	9.27E-07	9.44E-07
9.49E-07	9.60E-07	9.28E-07	9.46E-07
9.48E-07	9.59E-07	9.26E-07	9.44E-07
9.47E-07	9.57E-07	9.28E-07	9.44E-07
9.45E-07	9.56E-07	9.30E-07	9.44E-07
9.44E-07	9.57E-07	9.32E-07	9.44E-07

9.41E-07	9.59E-07	9.32E-07	9.44E-07
9.43E-07	9.59E-07	9.32E-07	9.45E-07
9.42E-07	9.59E-07	9.31E-07	9.44E-07
9.42E-07	9.58E-07	9.31E-07	9.44E-07
9.45E-07	9.57E-07	9.31E-07	9.44E-07
			9.44E-07

Table 7: The average of magnetic field produced by 3 straight rods with parallel power source

3 rods_dif source_1	3 rods_dif source_2	3 rods_dif source_3	Ave
1.57E-06	1.56E-06	1.57E-06	1.56E-06
1.56E-06	1.57E-06	1.56E-06	1.56E-06
1.57E-06	1.57E-06	1.57E-06	1.57E-06
1.57E-06	1.56E-06	1.57E-06	1.56E-06
1.57E-06	1.57E-06	1.57E-06	1.57E-06
1.56E-06	1.57E-06	1.56E-06	1.56E-06
1.57E-06	1.56E-06	1.57E-06	1.57E-06
1.56E-06	1.57E-06	1.57E-06	1.57E-06
1.56E-06	1.57E-06	1.56E-06	1.56E-06
1.57E-06	1.56E-06	1.57E-06	1.57E-06
1.56E-06	1.57E-06	1.57E-06	1.57E-06
1.57E-06	1.57E-06	1.56E-06	1.56E-06
1.57E-06	1.56E-06	1.57E-06	1.57E-06
1.56E-06	1.56E-06	1.57E-06	1.56E-06
1.57E-06	1.57E-06	1.56E-06	1.56E-06
			1.56E-06

Table 8: The average of magnetic field produced by 2 straight rods with series power source.

2 rods_series source_1	2 rods_series source_2	2 rods_series source_3	Ave
5.32E-07	5.23E-07	5.20E-07	5.25E-07
5.28E-07	5.15E-07	5.21E-07	5.21E-07
5.31E-07	5.24E-07	5.13E-07	5.22E-07
5.24E-07	5.22E-07	5.21E-07	5.22E-07
5.30E-07	5.22E-07	5.21E-07	5.24E-07
5.29E-07	5.24E-07	5.20E-07	5.24E-07
5.28E-07	5.16E-07	5.20E-07	5.21E-07
5.29E-07	5.24E-07	5.16E-07	5.23E-07
5.22E-07	5.25E-07	5.21E-07	5.23E-07
5.30E-07	5.25E-07	5.20E-07	5.25E-07
5.29E-07	5.27E-07	5.12E-07	5.23E-07
5.28E-07	5.23E-07	5.20E-07	5.24E-07
5.28E-07	5.27E-07	5.19E-07	5.25E-07
5.18E-07	5.27E-07	5.19E-07	5.21E-07
5.27E-07	5.20E-07	5.19E-07	5.22E-07
			5.23E-07

Table 9: The average of magnetic field produced by 3 straight rods with series power source

3 rods_series source_1	3 rods_series source_2	3 rods_series source_3	Ave
7.56E-08	7.52E-08	7.47E-08	7.52E-08
7.53E-08	7.51E-08	7.49E-08	7.51E-08
7.52E-08	7.51E-08	7.46E-08	7.50E-08
7.59E-08	7.52E-08	7.43E-08	7.52E-08
7.52E-08	7.51E-08	7.47E-08	7.50E-08
7.54E-08	7.51E-08	7.44E-08	7.50E-08
7.54E-08	7.51E-08	7.48E-08	7.51E-08
7.50E-08	7.50E-08	7.45E-08	7.48E-08
7.57E-08	7.50E-08	7.43E-08	7.50E-08
7.50E-08	7.53E-08	7.47E-08	7.50E-08
7.45E-08	7.56E-08	7.50E-08	7.51E-08
7.50E-08	7.55E-08	7.56E-08	7.53E-08
7.55E-08	7.52E-08	7.48E-08	7.52E-08
7.51E-08	7.54E-08	7.44E-08	7.50E-08
7.45E-08	7.49E-08	7.43E-08	7.46E-08
			7.50E-08

Discussion and conclusion:

Results in Table 5 to Table 9 were analyzed and plotted in the bar chart as shown in Figure 48. From the Figure 48, the three straight aluminium rods with **parallel power** source has the **highest value of magnetic field** produced ($1.56E^{-6}$). Parallel connection produce higher magnetic field because the connection provides the interference of waves where in this case, constructive interference was occurred. Two interfering waves have a displacement in the same direction and give a ‘super-crest’ which increase the value of magnetic field.

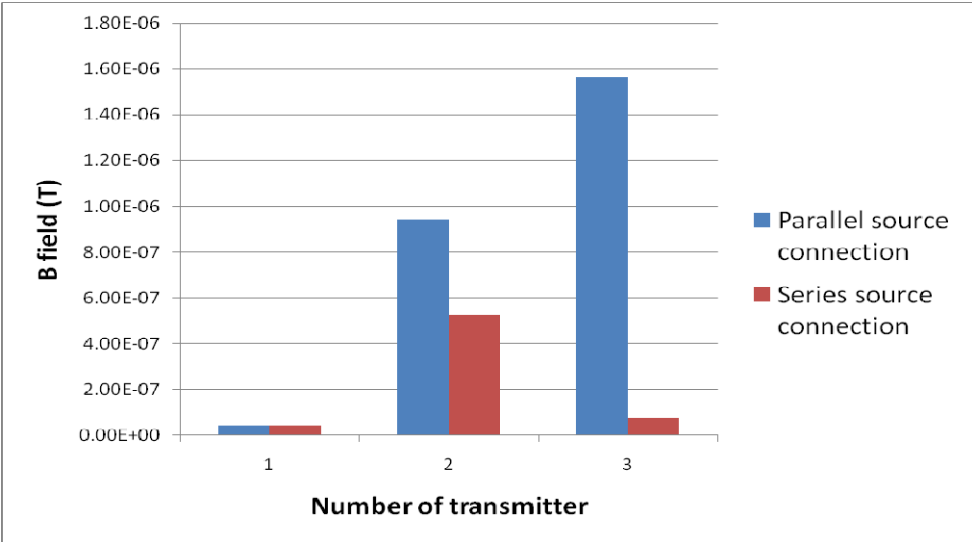


Figure 48: B-field for two source connection types

Experiment 4: Experimental Works on Aluminum Rod and Aluminum Wire

Equipments and materials used:

1. Function generator 80MHz
2. Curve aluminium rod with diameter of 10cm without magnetic feeder
3. Curve aluminium wire with diameter 10 cm without magnetic feeder
4. Wire clippers
5. Oscilloscope
6. Magnetic feeder (as receiver)

Description:

The fourth experiment was conducted in order to investigate the significant of material used for the transmitter design purpose which is between the aluminium rod and aluminium wire. For this experiment, aluminium curve rod (10cm diameter) and aluminium curve wire (10cm diameter) without magnetic feeder were used. Both were supplied with 80 MHz frequency. Oscilloscope was used to record the average received frequency that mostly appeared on the screen.

Results:

Table 10: Frequencies received by receiver for 1 curve aluminum rod and 1 curve aluminum wire (Frequencies are in MHz)

Readings	1 curve rod aluminum without m.feeder	1 curve aluminum wire without m.feeder
1	149.3	210.1
2	149.3	218.0
3	161.2	207.0
4	161.2	204.0
5	161.2	209.4
6	161.2	208.3
7	161.2	208.3
8	151.5	209.4
9	151.5	207.0
10	151.5	208.3
11	174.2	210.1
12	174.2	208.3
13	173.0	208.3
14	176.0	206.6
15	187.3	206.6
Average	162.9	208.6

Discussion and conclusion:

Based on the result in Table 10, with an aluminum curve wire without magnetic feeder, the value of frequency received is 208.6 MHz compare to aluminum rod, 162.9 MHz which shows that copper wire has a better ability to transmit higher frequency compared to the aluminum rod. This is due to the higher purity in aluminum wire rather than purity in aluminum rod.

The increment of frequency is about 28% if we use aluminum wire as the transmitter rather than aluminum rod.

Therefore, it was decided to design the transmitter in hexagon shape with the wire windings rather than to have transmitter with six connected rods.

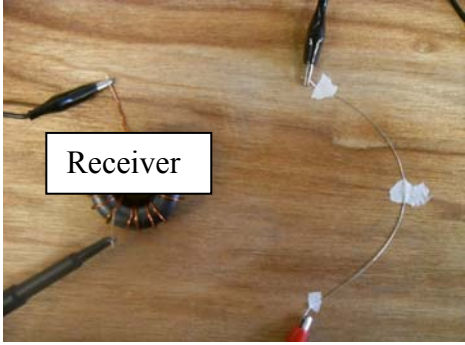
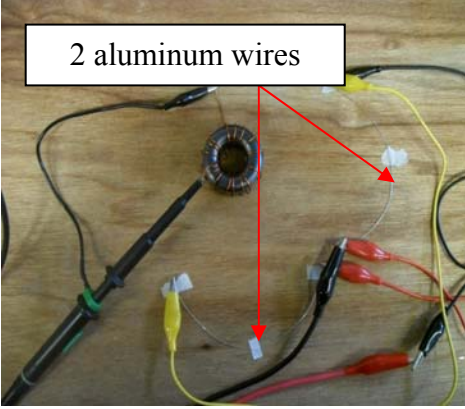
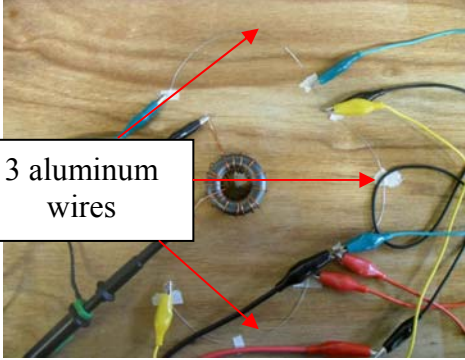
Experiment 5: Experimental Work on More Aluminum Curve Wires Used

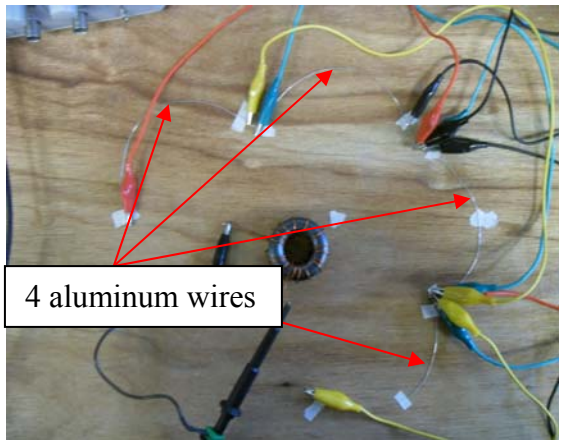
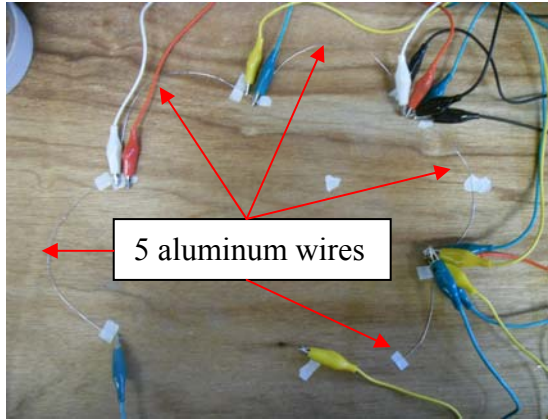
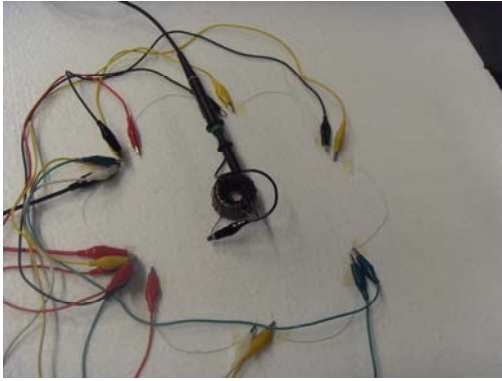
Equipments and materials used:

1. Function generator 80MHz
2. Eight aluminium wires with diameter 10 cm without magnetic feeder
3. Wire clippers
4. Oscilloscope
5. Magnetic feeder (as receiver)

Description:

Fifth experiment was done in order to figure out the ability of having more aluminium curve wires in increasing the value of transmitted frequency. In this experiment, 80 MHz frequency with parallel connection was supplied to the aluminium wires. The range of frequencies that mostly appeared on the oscilloscope was taken. 15 readings were recorded and the average of frequencies was calculated. The aluminium curve wires used were up to eight in numbers.

	<p>1 aluminum wire</p>
	<p>2 aluminum wires</p>
	<p>3 aluminum wires</p>

 <p data-bbox="500 527 760 583">4 aluminum wires</p> <p data-bbox="699 737 824 772">Figure 52</p>	<p data-bbox="1068 380 1222 447">4 aluminum wires</p>
 <p data-bbox="597 1066 865 1123">5 aluminum wires</p> <p data-bbox="699 1262 824 1297">Figure 53</p>	<p data-bbox="1068 961 1222 1029">5 aluminum wires</p>
 <p data-bbox="699 1717 824 1753">Figure 54</p>	<p data-bbox="1068 1451 1222 1518">6 aluminum wires</p>

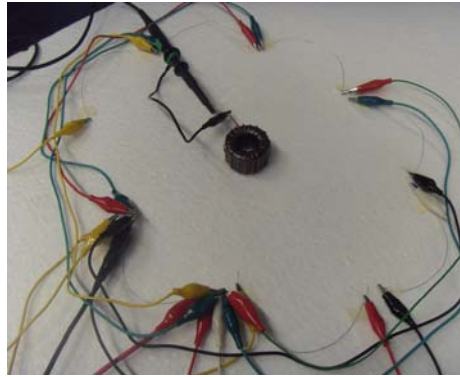


Figure 55

7 aluminum
wires

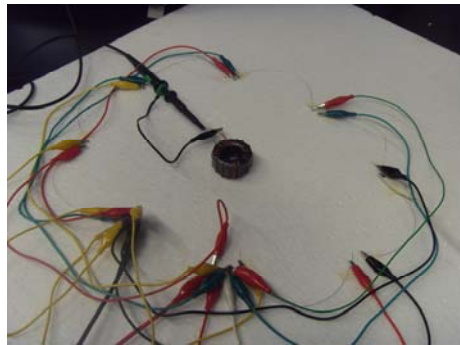


Figure 56

8 aluminum
wires

Result:

Table 11: Frequencies received by receiver for 1 until 8 curve aluminum wires
(Frequencies are in MHz)

Readings	1 curve	2 curves	3 curves	4 curves	5 curves	6 curves	7 curves	8 curves
1	210.1	295.7	331.1	434	549.5	555.5	555.6	555.6
2	218	282.5	331.1	434	549.5	555.5	555.6	555.6
3	207	267.2	333.1	434	537.3	555.5	555.6	555.6
4	204	279.3	333.1	431.3	537.3	568.5	555.6	555.6
5	209.4	267.2	328.3	431.3	537.3	568.5	555.6	568.2
6	208.3	267.2	328.3	431.3	561.4	598.4	555.6	568.2
7	208.3	294.7	367	427	531.3	625	555.6	568.2
8	209.4	279.3	367	427	595.6	625	555.6	568.2
9	207	279.3	314.5	423.7	625	625	555.6	568.2
10	208.3	294.7	326.8	442.7	625	657	568.2	568.2
11	210.1	295.7	387	403	641.2	657	568.2	543.5
12	208.3	279.3	362.2	438.8	641.2	657	568.2	602.4
13	208.3	279.3	357.5	420	657.7	641.8	567.5	602.4
14	206.6	279.3	340	471	657.7	641.8	537	657.2
15	206.6	279.3	331.1	480	648	609	602	568.2
Average	208.6	281.3	342.54	435.3	593.0	609.4	560.8	573.7

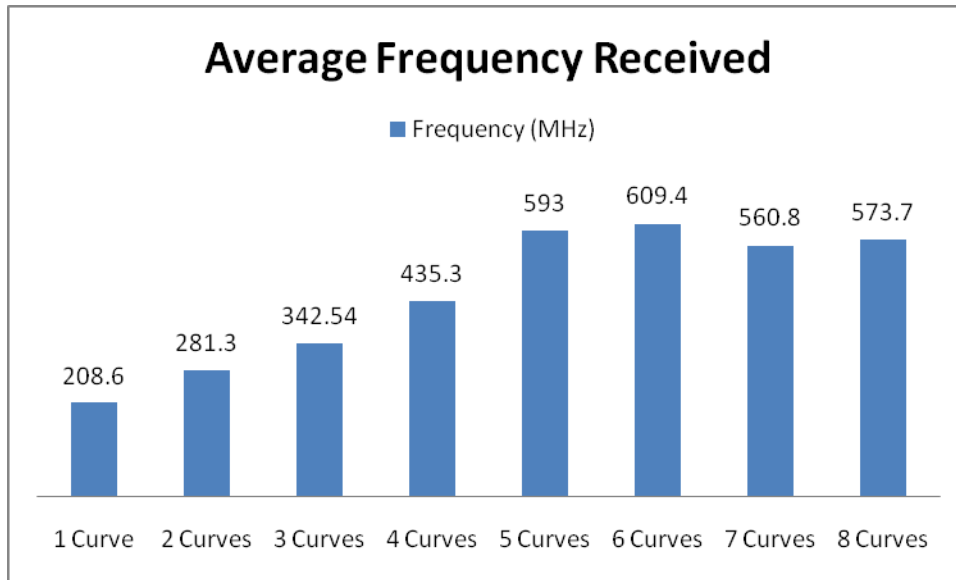


Figure 57: The average frequency received

Discussion and Conclusion:

From the results shown in Figure 57, the increment of received frequency for each increment of aluminum wire was about 22% to 35%. For example, by using one aluminum wire, the frequency received was 208.65 MHz and for two aluminum wires, the frequency received was 281.33 MHz which give about 34.5% of increment.

The relevant number of aluminum wire to be used based on the results is by having six aluminum wires because the frequency transmitted for more than six wires will be equally the same values; this is about 567.227 MHz in average.

Experiment 6: Experiment Work on Nanoparticle Magnetic Feeder and Amplifier.

Equipments and materials used:

1. Function generator 1KHz
2. Designed transmitter
3. Wire clippers
4. Fluxgate Magnetometer
5. Nanoparticle Magnetic feeder
6. Power amplifier

Description:

Further experiment was done in order to evaluate the significant of using nanoparticle magnetic feeder and amplifier with the designed EM transmitter in term of B-field transmitted. The experiments were done in three conditions;

- I. Transmitter without amplifier and magnetic feeders
- II. Transmitter with amplifier
- III. Transmitter with amplifier and magnetic feeders

For the first experiment the transmitter was connected in parallel connection with the 1 KHz frequency supply and left for 30 minutes. The fluxgate magnetometer was placed 25cm from the running transmitter and the B field transmitted data was saved and analyzed. The same procedures were considered for the other two conditions where amplifier and nanoparticle magnetic feeders were used.

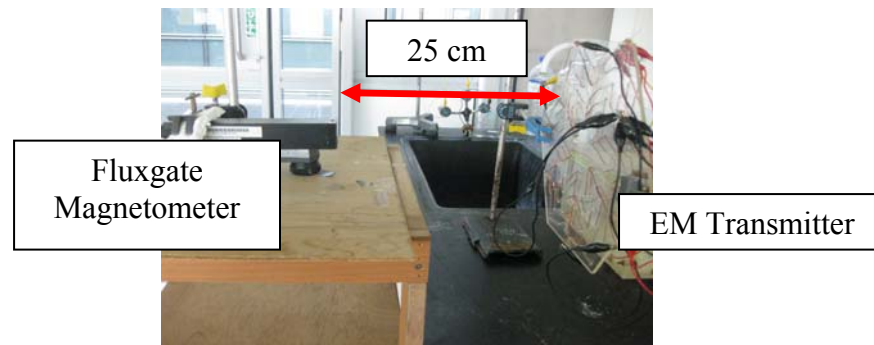


Figure 58: Experiment Set up to Evaluate the EM Transmitter When Using NanoParticle Magnetic Feeders and Power Amplifier

Results:

Table 12: B field transmitted without amplifier and magnetic feeder

without Mf&_1	without Mf&_2	without Mf&_3	Average
4.08E-09	4.13E-09	4.02E-09	4.07E-09
4.42E-09	4.01E-09	4.27E-09	4.23E-09
4.13E-09	3.97E-09	4.25E-09	4.11E-09
4.33E-09	4.18E-09	4.32E-09	4.27E-09
4.64E-09	3.67E-09	4.47E-09	4.26E-09
4.07E-09	4.46E-09	4.13E-09	4.22E-09
4.26E-09	4.19E-09	3.84E-09	4.09E-09
4.28E-09	4.09E-09	4.29E-09	4.22E-09
4.07E-09	4.07E-09	4.39E-09	4.18E-09
4.34E-09	4.14E-09	4.33E-09	4.27E-09
4.36E-09	4.22E-09	4.20E-09	4.26E-09
4.02E-09	4.29E-09	3.94E-09	4.09E-09
3.84E-09	4.34E-09	4.69E-09	4.29E-09
4.21E-09	4.17E-09	4.52E-09	4.30E-09
4.26E-09	4.10E-09	4.13E-09	4.16E-09
3.99E-09	4.41E-09	4.45E-09	4.28E-09
4.16E-09	4.21E-09	4.51E-09	4.30E-09
4.01E-09	4.29E-09	4.53E-09	4.28E-09
4.13E-09	4.75E-09	4.41E-09	4.43E-09
4.39E-09	4.37E-09	4.22E-09	4.33E-09
4.65E-09	4.05E-09	4.45E-09	4.38E-09
4.46E-09	4.10E-09	4.31E-09	4.29E-09
4.26E-09	4.46E-09	4.15E-09	4.29E-09
4.21E-09	4.22E-09	4.11E-09	4.18E-09
4.26E-09	3.84E-09	4.00E-09	4.03E-09
4.37E-09	4.17E-09	4.32E-09	4.28E-09
4.14E-09	3.82E-09	4.47E-09	4.14E-09
4.22E-09	4.62E-09	4.23E-09	4.36E-09
4.32E-09	4.42E-09	4.57E-09	4.43E-09
4.40E-09	4.30E-09	3.95E-09	4.22E-09
4.30E-09	4.19E-09	4.59E-09	4.36E-09
			4.25E-09

Table 13: B field transmitted with amplifier

with amp_1	with amp_2	with amp_3	Average
5.22E-09	6.39E-09	6.04E-09	5.88E-09
6.02E-09	5.78E-09	6.43E-09	6.08E-09
6.12E-09	4.63E-09	6.07E-09	5.61E-09
6.37E-09	3.43E-09	4.84E-09	4.88E-09
5.17E-09	2.35E-09	3.96E-09	3.83E-09
4.03E-09	3.10E-09	2.83E-09	3.32E-09
2.53E-09	4.23E-09	2.72E-09	3.16E-09
3.01E-09	5.16E-09	3.94E-09	4.04E-09
3.80E-09	5.93E-09	5.76E-09	5.16E-09
4.97E-09	6.13E-09	6.00E-09	5.70E-09
6.43E-09	6.54E-09	6.48E-09	6.48E-09
6.29E-09	5.99E-09	6.43E-09	6.24E-09
6.39E-09	4.57E-09	5.71E-09	5.56E-09
5.58E-09	3.59E-09	4.64E-09	4.60E-09
4.95E-09	2.32E-09	3.56E-09	3.61E-09
2.80E-09	2.86E-09	2.38E-09	2.68E-09
2.11E-09	4.23E-09	3.15E-09	3.16E-09
4.05E-09	5.22E-09	4.30E-09	4.52E-09
4.71E-09	5.86E-09	5.76E-09	5.44E-09
5.60E-09	6.24E-09	6.00E-09	5.95E-09
6.42E-09	6.15E-09	6.10E-09	6.22E-09
6.34E-09	5.76E-09	6.36E-09	6.15E-09
5.96E-09	4.56E-09	5.19E-09	5.24E-09
4.84E-09	3.52E-09	4.34E-09	4.23E-09
3.94E-09	2.59E-09	2.57E-09	3.03E-09
2.75E-09	2.83E-09	2.86E-09	2.81E-09
2.99E-09	4.29E-09	3.41E-09	3.56E-09
4.21E-09	5.34E-09	4.71E-09	4.75E-09
5.38E-09	6.13E-09	5.41E-09	5.64E-09
6.05E-09	6.22E-09	6.30E-09	6.19E-09
6.05E-09	6.20E-09	6.19E-09	6.15E-09
			4.83E-09

Table 14: B field transmitted with feeders

with m.feeder_1	with m.feeder_2	with m.feeder_3	Average
2.06E-08	3.04E-08	2.26E-08	2.45E-08
2.62E-08	3.23E-08	2.91E-08	2.92E-08
3.57E-08	3.20E-08	3.31E-08	3.36E-08
3.58E-08	2.65E-08	3.41E-08	3.22E-08
3.07E-08	2.23E-08	3.19E-08	2.83E-08
2.22E-08	2.71E-08	2.96E-08	2.63E-08
2.77E-08	3.78E-08	2.73E-08	3.09E-08
4.06E-08	4.65E-08	2.07E-08	3.59E-08
4.42E-08	4.79E-08	3.20E-08	4.13E-08
4.12E-08	4.58E-08	3.96E-08	4.22E-08
3.23E-08	3.95E-08	4.71E-08	3.96E-08
2.88E-08	3.36E-08	5.56E-08	3.93E-08
4.62E-08	3.53E-08	5.73E-08	4.62E-08
5.15E-08	5.18E-08	5.44E-08	5.26E-08
5.12E-08	6.03E-08	4.67E-08	5.27E-08
4.21E-08	6.57E-08	3.83E-08	4.87E-08
3.27E-08	6.69E-08	4.13E-08	4.70E-08
4.53E-08	6.33E-08	6.52E-08	5.79E-08
5.72E-08	4.75E-08	8.37E-08	6.28E-08
5.77E-08	4.26E-08	9.40E-08	6.48E-08
5.40E-08	5.72E-08	1.00E-07	7.04E-08
4.41E-08	7.81E-08	1.01E-07	7.44E-08
4.08E-08	8.95E-08	9.27E-08	7.43E-08
6.24E-08	8.92E-08	7.22E-08	7.46E-08
6.84E-08	8.28E-08	5.57E-08	6.90E-08
6.91E-08	7.21E-08	6.35E-08	6.82E-08
6.44E-08	5.50E-08	7.96E-08	6.63E-08
4.40E-08	6.56E-08	8.61E-08	6.52E-08
6.73E-08	8.99E-08	8.55E-08	8.09E-08
8.58E-08	1.04E-07	7.78E-08	8.91E-08
9.21E-08	1.10E-07	6.18E-08	8.80E-08
			5.34E-08

Table 15: B field transmitted with amplifier and feeder

with feeder+amp_1	with feeder+amp_2	with feeder+amp_3	Average
9.03E-09	9.19E-09	9.23E-09	9.15E-09
9.35E-09	9.22E-09	8.83E-09	9.14E-09
9.82E-09	9.42E-09	8.67E-09	9.30E-09
9.10E-09	9.26E-09	8.58E-09	8.98E-09
8.72E-09	8.57E-09	7.42E-09	8.24E-09
8.59E-09	8.33E-09	7.33E-09	8.08E-09
7.92E-09	8.14E-09	7.26E-09	7.77E-09
7.86E-09	7.86E-09	7.45E-09	7.72E-09
7.20E-09	7.05E-09	7.62E-09	7.29E-09
7.42E-09	7.27E-09	7.29E-09	7.33E-09
7.13E-09	7.15E-09	8.65E-09	7.65E-09
7.41E-09	7.85E-09	8.41E-09	7.89E-09
7.94E-09	8.85E-09	8.78E-09	8.53E-09
8.57E-09	9.08E-09	8.83E-09	8.82E-09
8.77E-09	9.14E-09	9.08E-09	8.99E-09
9.43E-09	9.16E-09	9.15E-09	9.25E-09
9.28E-09	9.88E-09	8.92E-09	9.36E-09
9.12E-09	8.99E-09	9.09E-09	9.07E-09
8.95E-09	9.18E-09	8.72E-09	8.95E-09
9.31E-09	8.35E-09	8.45E-09	8.70E-09
8.85E-09	7.64E-09	8.29E-09	8.26E-09
8.45E-09	8.17E-09	7.82E-09	8.15E-09
8.18E-09	7.34E-09	7.44E-09	7.65E-09
7.87E-09	7.38E-09	7.12E-09	7.45E-09
7.24E-09	7.28E-09	7.12E-09	7.21E-09
7.00E-09	7.83E-09	7.42E-09	7.42E-09
7.61E-09	8.49E-09	7.98E-09	8.03E-09
7.55E-09	8.68E-09	8.05E-09	8.09E-09
7.82E-09	9.40E-09	8.28E-09	8.50E-09
8.57E-09	9.39E-09	9.39E-09	9.12E-09
8.63E-09	9.18E-09	9.01E-09	8.94E-09
			8.36E-09

Discussion and Conclusion:

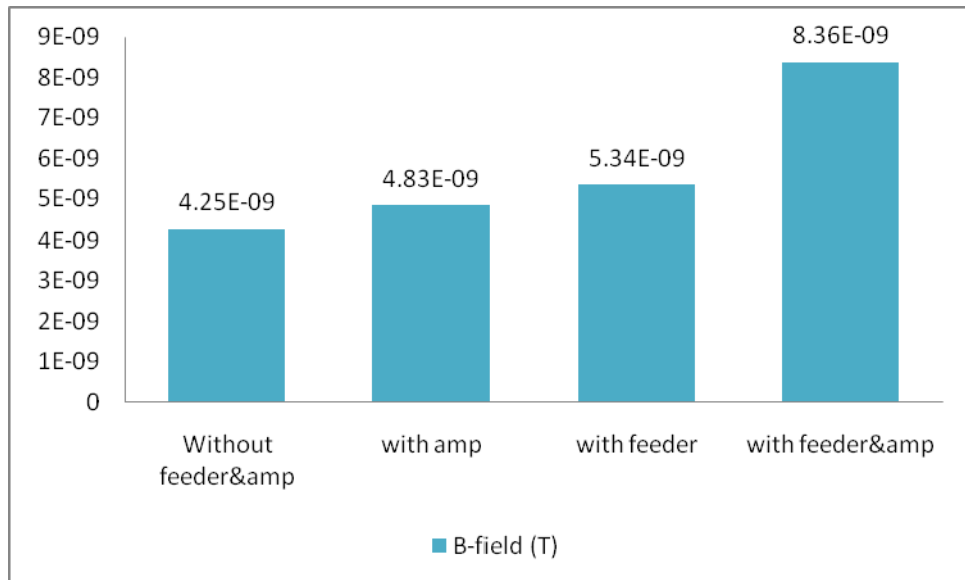


Figure 59: B field transmitted (T)

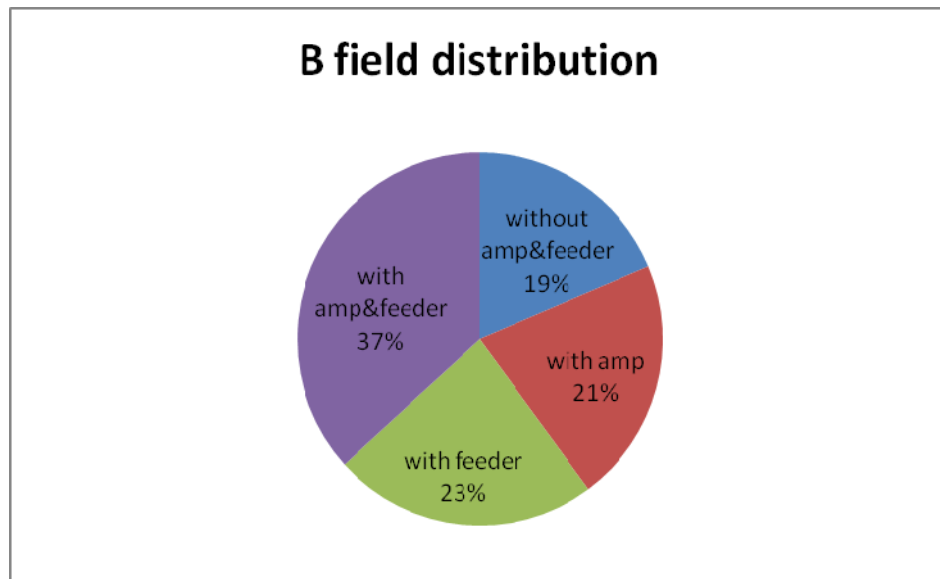


Figure 60: B field distribution (%)

From the results shown in the Figure 59, the transmitter's B-field distribution is higher with the existence of the amplifier and nanoparticle magnetic feeders, where the transmitter's B-field is increased by 96.7%. The B-field of the transmitter was increased because the amplifier has amplifies the current flow in the copper conductor wire which then govern to the higher B-field production, while the magnetic feeders are function as an additive to the additional of B-field produced by the transmitter.

From Figure 59 transmitter with nanoparticle magnetic feeders shows the increment about 25.6% while transmitter with amplifier has the increment of 13.67%. This is show that nanoparticle magnetic feeders and amplifier are suitable to be used with the transmitter.

Figure 60 shows by the percentage representation that the increment of magnetic field strength is the highest when we use magnetic feeders together with the amplifier.

Experiment 7: Porosity and Permeability Test for Core Sample.

Equipments and materials used:

1. Helium Porosimeter
2. Weighing Apparatus
3. Caliper

Description:

This experiment was conducted in order to evaluate the core sample characteristic which are included the porosity, pore volume and also the permeability. The core sample which was firstly has been measured its wide, height, thickness and weight (using calliper), was then placed into the porosimeter holder. Helium gas has been applied with high pressure and then all the data were taken after 30 minutes running the test.

Result:

Table 16: Measurements from Porosity Test

Data	Measurement
Air Permeability(mD)	567.80
Pore Volume (cc)	17.77
Porosity (%)	21.18
grain Volume(cc)	66.13
bulk Volume(cc)	83.89
grain density(g/cc)	2.59
bulk density (g/cc)	2.04

Discussion and Conclusion:

These measurements are very important in order to investigate and understand about the relationship of porosity, pore volume and permeability with the oil recovery calculation. Higher pore volume would cause to the bigger volume of the connected pores in the core sample which means that more crude oil can be placed inside compared to the smaller pore volume.

Experiment 8: Core Flooding

Equipments and materials used:

1. Core Flooding Machine
2. Weighing Apparatus
3. Crude Oil with density of 0.811g/cc
4. Brine Water with density of 1.018g/cc

Description:

This experiment was conducted in order to prepare the core sample with the crude oil and brine. There were four main processes that involved in this experiment. The first process was to be the saturation of the core sample with the brine water for 24 hours. This procedure's purpose was to make the core sample was fully saturated with the brine and to ensure that there was no air inside the core.

The other three processes were carried in the core flooding machine where the second process was about to have second brine water injection into the core sample. Third process was to be the crude oil injection and fourth process was again the brine water injection. Figure 61 shows the parameter involved while doing this experiment where the inlet part was used to inject the brine and crude oil. Figure 61 also shows the pressure and temperature involved while preparing the core sample with brine and crude oil.

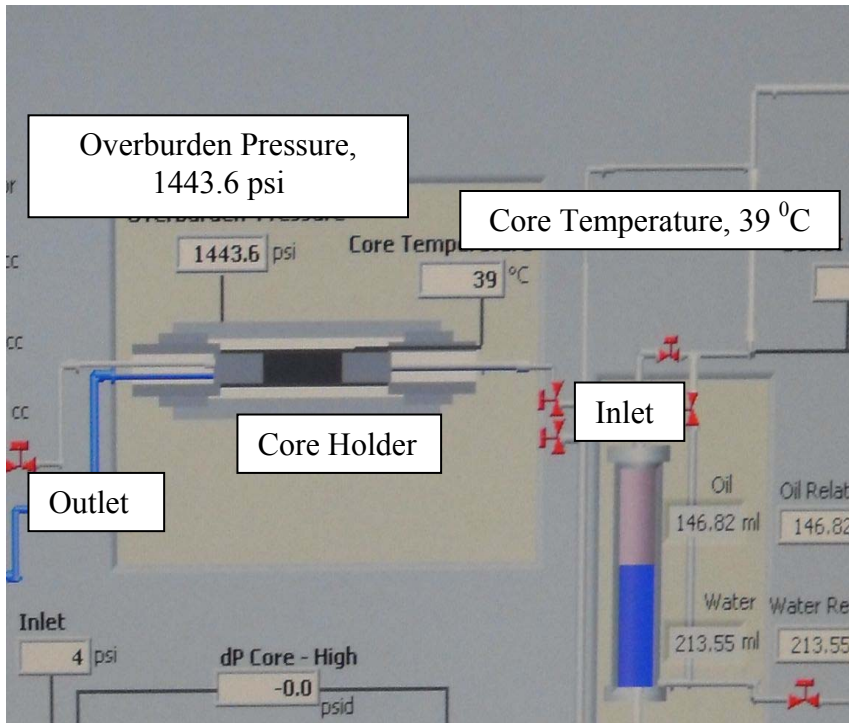


Figure 61: Parameters involved in Core Flooding Process

Results:

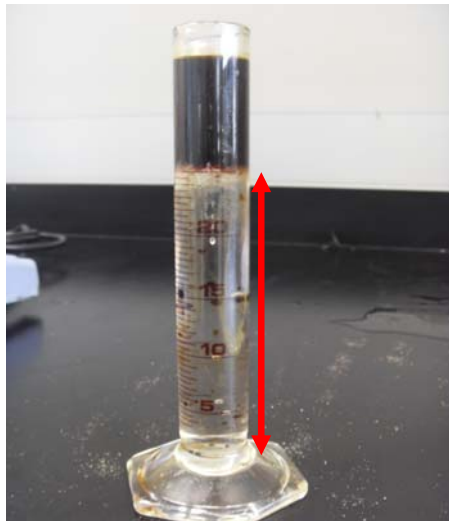


Figure 62: Brine Water after Crude Oil Injection

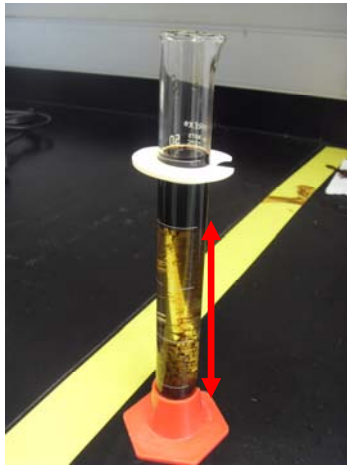


Figure 63: Brine water after Second Brine Water Injection Process

Table 17: Core Flooding OOIP and ROIP

Data	Measurement
Porosity (%)	21.18
Pore Volume (cc)	17.77
OOIP (ml)	12
ROIP (ml)	6.2

Result and Discussion:

Second brine injection in the core sample using the Core Flooding Machine was to confirm that there was no air at all inside the core. Another purpose of having second brine water injection was as a measurement purpose to calculate the crude oil that would be placed inside the core sample where the volume crude oil placed in the core sample in the third process would be the same as the volume of brine water that came out from the outlet (see figure 62). The oil placed inside the core sample at this process was called as the Original Oil In place (OOIP).

The third brine injection purpose was to put the core rock into the real situation where the real reservoir would consist of crude oil with the brine water. In this process, the injection of brine water was stopped once we notice that there was no more oil coming out from the outlet part. The remaining oil inside the core sample was calculated and the called as the Residue Oil In Place (ROIP). ROIP was calculated by subtracting the water displacement after the process of brine injection from the OOIP volume (see Figure 63).

Table 17 shows that the value of OOIP and ROIP measurements.

Experiment 9: Oil Recovery Using EM waves

Equipments and materials used:

1. 5 MHz function generator
2. DC power supply
3. Power Amplifier
4. Temperature controller
5. Weighing apparatus
6. Tank
7. Fluxgate Magnetometer

Description:

This experiment was carried out in order to calculate the oil recovery by using the EM waves method where the designed EM Transmitter become the main tool to have the recovery. The experiment setup is shown in Figure 64. The core sample was left to be exposed to the EM waves for 36 hours where the weight of core sample was taken at 2,4,10,12,18,24 and 36 hours.

Set Up:

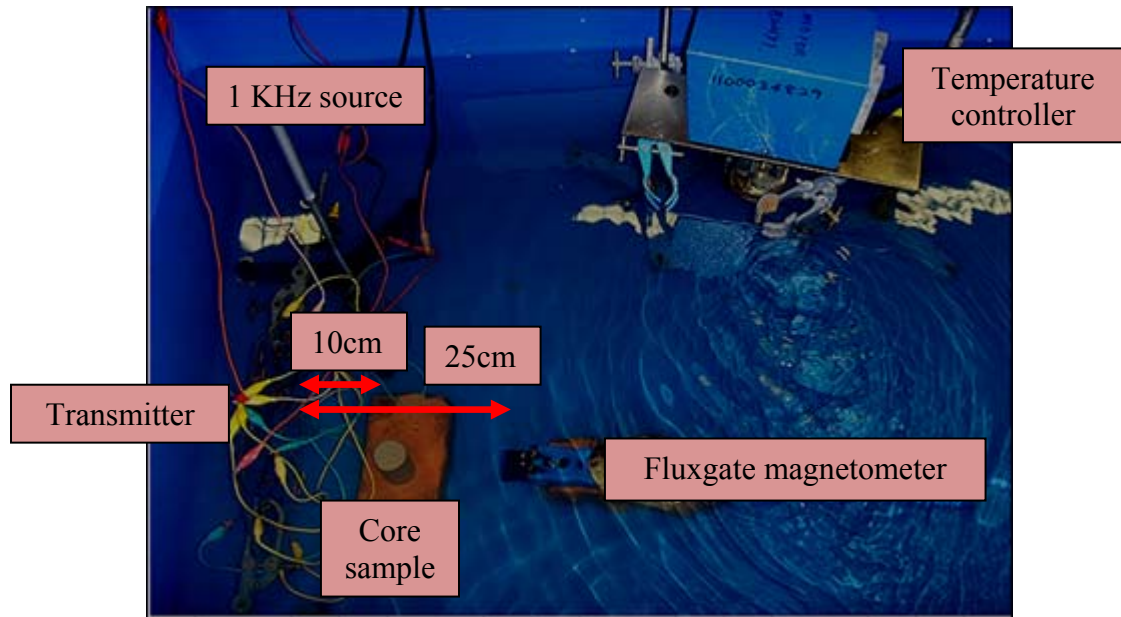


Figure 64: Experiment set up for oil recovery

Result and Discussion:

This experiment was consist of two main parts which were including the analysis used to prove that the fluxgate magnetometer could be one of the calculation method of the recovery using EM waves and the another part was the analysis about the oil recovery.

The analysis in the oil recovery was then divided into two parts which were the analysis from the fluxgate magnetometer data and second part was the analysis from the core sample weight measurements. Both methods of recovery gave approximately the same values of recovery percentage.

Part 1: To Prove the Potential of Fluxgate Magnetometer to be a Tool of Oil Recovery Calculation.

Table 18: B field distribution in three conditions

without_c.Rock	empty_c.Rock	flooded_c.Rock(Ave)
2.71E-08	2.72E-08	4.5E-08

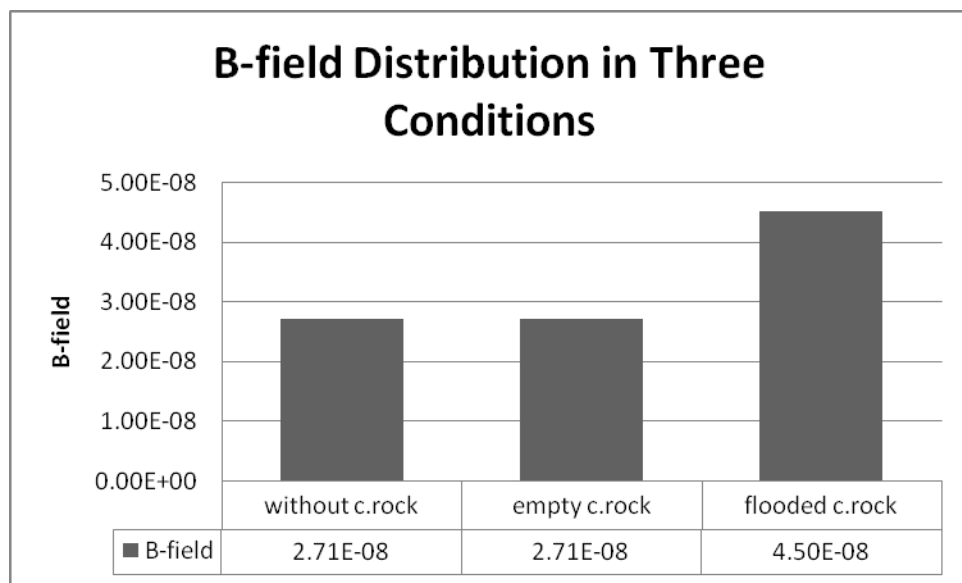


Figure 65: B field distribution in three conditions

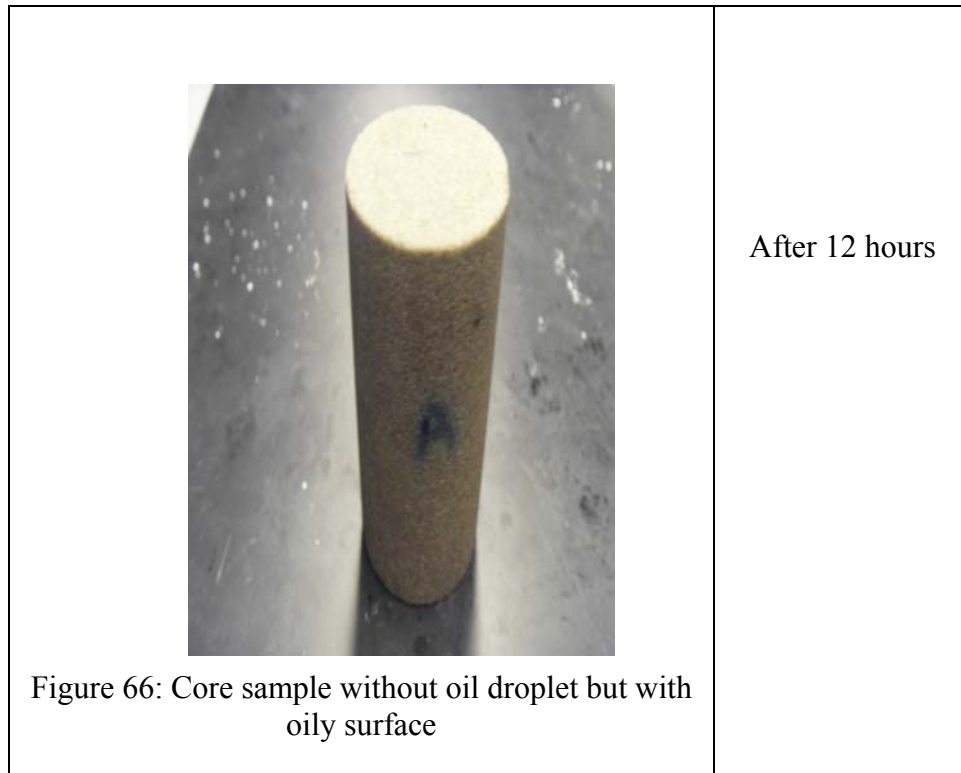
The B field transmitted by the transmitter was evaluated base on three conditions which are included;

- a. B field propagation direct to the fluxgate magnetometer (without core rock)
- b. B field propagation through the empty core sample (no crude oil and brine inside)

- c. B field propagation through the flooded core sample (with crude oil and brine inside).

From Figure 65, we could see that the intensity of B field for both conditions without and with empty core rock is the same while intensity of B field through the flooded core rock was slightly higher than the other conditions. The increment on the B-field measurement shows that Fluxgate magnetometer could detect the crude oil inside core rock samples and can be a tool to calculate the oil recovery using EM waves.

Part 2: Analysis on the Oil Recovery





After 18 hours

Figure 67: Core Sample with a little oil droplets



After 24 hours

Figure 68: Core sample with More Oil Droplets



After 36 hours

Figure 69: Core Sample with Increasing Number of Oil Droplets

Table 19: B field distribution in core sample from 0 hour to 36 hours

0 hr	2hrs	4hrs	10hrs	12hrs	18hrs	24hrs	36hrs
2.71E-08	3.77E-08	4.09E-08	4.19E-08	3.77E-08	3.46E-08	3.32E-08	3.32E-08

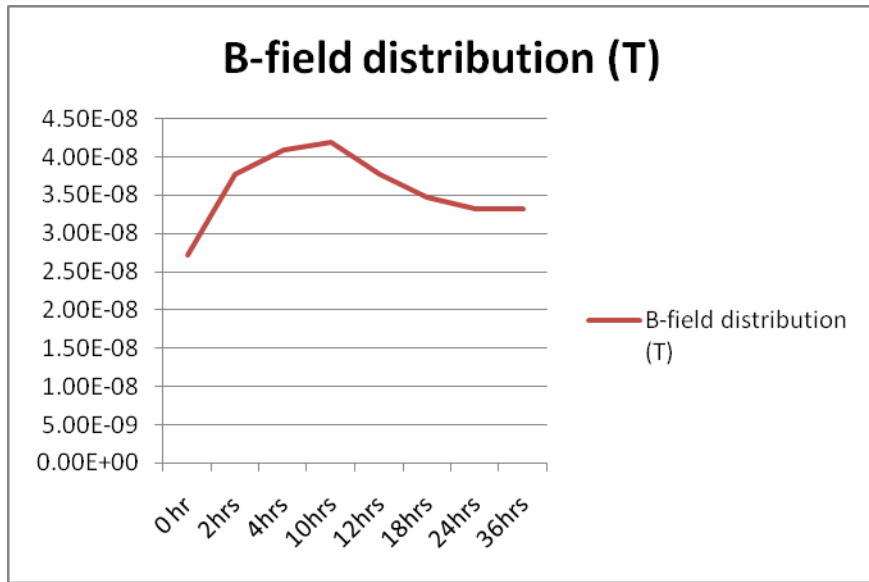


Figure 70: B field distribution through the core sample

From Figure 70, it shows that the Fluxgate magnetometer detects the existence of crude oil in the core sample up to 10 hours and after that the B-field detection values were decreasing due to the oil recovery after 12 hours which means less crude oil was detected after the recovery.

From 0 hour up to 10 hours, the B-field detected was increasing to 4.19E-08 and after that the B field decreasing due to the oil that came out. This analysis also proving that the detection of B field by the fluxgate magnetometer could be one of the methods to estimate the oil recovery from the core sample.

The remaining oil was represented by the B-field value after 36 hours (3.32E-08) and the residue oil inside the core sample was represented by the maximum value of B-field (4.19E-08).

Calculation to Find the Recovery Using Fluxgate Magnetometer Data:

Table 20: Average B-field through core sample

Residue Oil (up to 10 hrs)	Remaining oil(after 36 hours)
4.19E-08	3.32E-08

The residue oil in core sample is calculated by making a corresponding value of B-field up to 10 hours (before oil is coming out) with the residue oil in volume (6.2ml).

Where;

Table 21: Core Sample Data

Data	Measurement
Original Oil In Place (OOIP) (ml)	12
Produced oil after flooding (ml)	5.8
Residue Oil In Place (ROIP) (ml)	6.2

$4.19E^{-8}$ is correspond to the 6.2ml

Therefore;

The remaining oil in core sample after 36 hours is $\frac{3.32E^{-8}}{4.19E^{-8}} * 6.2ml = 4.9ml$

Recovered Oil = 6.2ml-4.9ml

$$= 1.3ml$$

$$\text{Recovery} = \frac{1.3ml}{12ml} * 100 = 10.83\% \text{ OOIP}$$

The oil recovery calculated using the fluxgate magnetometer B-field data was to be 10.83% OOIP.

Calculation to Find the Recovery Using Weighing Method:

Table 22: Core sample measurements

Data	Measurement
Dry weight before flooding(g)	173.5354
Weight after flooding (g)	187.945
Original Oil In Place (OOIP) (ml)	12
Produced oil after flooding (ml)	5.8
Residue Oil In Place (ROIP) (ml)	6.2
Weight after 36 hours with EM waves (g)	186.4
weight after dried in oven (2 days) (g)	177.321

$$\text{Remaining Oil in core sample} = \frac{177.321g - 173.5354g}{0.811 \frac{g}{ml}} = 4.67ml$$

Residue Oil in core sample before exposed to EM waves= 6.2ml

Recovered Oil = 6.2ml-4.67ml

$$= 1.53ml$$

$$\text{Recovery} = \frac{1.53ml}{12ml} * 100 = 12.71\% \text{ OOIP}$$

The recovery was calculated to be 12.71% by using the weighing method.

CHAPTER 5

CONCLUSION & RECOMMENDATION

5.1 Conclusion

As the conclusion, the simulations and experiments done were successful and fulfill the objectives which are to design and to construct an EM transmitter to demonstrate the behavior of EM waves on a core sample to improve the oil mobility and thus to have at least 10% of recovery. The designed EM transmitter with six segments (hexagon), 1m curve copper wire windings for each segment with separate six frequency sources is proven able to recover 10-12% of oil within 36 hours by only supplied with 1 KHz of frequency.

5.2 Major Finding

Through this project, we had successfully recovered about 10-12% of oil using EM waves where this method is the first conducted in UTP and PETRONAS.

5.3 Recommendation

Potential work that can be done are first to further study on the distance between the transmitter's sources where it should be varied in order to optimize the construction of Electromagnetic waves produced. Besides having a proper distance of the transmitter's sources, the transmitter windings also could be increased so that more B-field can be produced. Smaller transmitter with powerful EM wave's transmission also could be designed by using nano carbon wires as the transmitter's windings.

The authors also suggested that for future experiment, the frequency sources to the transmitter should be varied and at the same time maintain the temperature of brine water to be 37⁰C. Lower and upper frequencies than 1 KHz should be applied and study on the significant of having those frequencies to the oil recovery.

The position of core rock and transmitter could also be varied to horizontal and vertical condition in order to investigate the effect of positioning to the recovery.

REFERENCES

- [1] Enhanced Oil Recovery Scoping Study, EPRI, Palo Alto, CA: 1999. TR-113836
- [2] Gary Dolberry on Enhanced Oil RecoveryBy OrangeCast
- [3] http://www.rigzone.com/training/insight.asp?insight_id=313&c_id=
- [4] <http://www.ees.lanl.gov/ees11/geophysics/stimulation/fossil.shtml>
- [5] Swapan Das, SPE, Marathon Oil Corporation, Electro-Magnetic Heating in Viscous Oil Reservoir
- [6] *August 2000*, Journal of Canadian Petroleum Technology, In Situ Electromagnetic Heating for Hydrocarbon Recovery and Environmental Remediation, *volume 39, No 8*
- [7] Enhanced Oil Recovery of Ugnu Tar Sands of Alaska Using Electromagnetic Heating with Horizontal Wells, M.R.Islam, EMERTEC Developments Inc. and S.S Wadader and A.Bansal, U.of Alaska Fairbanks
- [8] Fawwaz T.Ulaby, Magnetostatics, Electromagnetics for Engineers, Pearson Education International, *The University of Michigan*, (2005)
- [9] Electromagnetic Waves from Maxwell's Equations, Peter Signell, Michigan State University.
- [10] http://galileoandstein.physics.virginia.edu/more_stuff/Maxwell_Eq.html
- [11] Karl J.Ellefsen, Jared D.Abraham, David L. Wright and Aldo T.Mazzela. Numerical Study of Electromagnetic Waves Generated by a Prototype Dielectric Lagging Tool.
- [12] Shahbender, Babah; Wendt, Frank.S; Gordon, Irwin; Gries, Robert J. Television Receiver Ferroresonant High Voltage Power Supply Using Temperature Stable Core Material.
- [13] Alex Becker, Ki Ha Lee, and Lou Reginato. Field Test of a Wideband Downhole EM Transmitter.
- [14] <http://www.cflhd.gov/agm/about/index.htm>
- [15] Marine EM Methods Steven Constable
< <http://www.searchanddiscovery.net/documents/2005/constable/index.htm>>

- [16] Development of A Powerful EM Transmitter, Nur Azliza Ahmad,Universiti Teknologi PETRONAS
- [17] http://astro-canada.ca/_en/a2313.html
- [18] A scaled experiment for the verification of the SeaBed Logging method L.O. Løseth, H.M. Pedersen, T. Schaug-Pettersen, S. Ellingsrud and T. Eidesmo, Volume 64, Issues 3-4, 21 April 2008, Pages 47-55
- [19] <http://www.physicsclassroom.com/mmedia/waves/em.cfm>
- [20] ProjectPHYSNET-Physics Bldg-Michigan State University- East Lansing, MI
- [21] Harvesting Oil from the Earth Contributed by: Integrated Teaching and Learning Program, College of Engineering, University of Colorado at Boulder
- [22] New Energy Forms-Tesla Wireless Technology, April 2007
- [23] www.leonardo-energy.org
- [24] <http://dmseg5.case.edu/Classes/EMSE201/overheads/ElecCond.pdf>
- [25] <http://liquidgoldinternational.com/information-on-enhanced-oil-recovery/enhanced-oil-recovery-2>
- [26] Pilot Testing of a Radio Frequency Heating System for Enhanced Oil Recovery from Diatomaceous Earth. R.S KA, Technologies Inc.,and M.F.Fontaine, Texaco EPTD
- [27] D Alan. Chave, Steven C. Constable, and R. Nigel Edwards "Electrical Exploration Methods For The Seafloor" Electromagnetic Methods in Applied Geophysics, SEG, [1982].
- [28] L.O. Løseth, H.M. Pedersen, S. Pettersen, T. S. Ellingsrud, T. Eidesmo, "A scaled experiment for the verification of the SeaBed Logging method," Journal of Applied Geophysics, vol. 64, pp. 47–55, [2008].

APPENDIX A
TABLES FOR EXPERIMENT 9

Table A: B field without core rock

Without CR_1	Without CR_2	Without CR_3	Average
2.37E-07	2.49E-07	2.54E-07	2.47E-07
1.89E-08	2.62E-08	2.53E-08	2.35E-08
1.49E-08	2.23E-08	2.81E-08	2.17E-08
8.80E-09	1.78E-08	2.84E-08	1.83E-08
3.48E-09	1.24E-08	2.86E-08	1.48E-08
8.39E-09	6.10E-09	2.73E-08	1.39E-08
1.33E-08	7.58E-09	2.45E-08	1.51E-08
1.86E-08	1.40E-08	2.08E-08	1.78E-08
2.24E-08	1.92E-08	1.62E-08	1.93E-08
2.63E-08	2.35E-08	9.93E-09	1.99E-08
2.79E-08	2.63E-08	4.06E-09	1.94E-08
2.81E-08	2.78E-08	8.54E-09	2.15E-08
2.81E-08	2.83E-08	1.40E-08	2.34E-08
2.74E-08	2.75E-08	1.94E-08	2.48E-08
2.49E-08	2.48E-08	2.41E-08	2.46E-08
2.27E-08	2.07E-08	2.69E-08	2.34E-08
1.83E-08	1.48E-08	2.80E-08	2.04E-08
1.29E-08	8.17E-09	2.88E-08	1.66E-08
7.43E-09	5.30E-09	2.81E-08	1.36E-08
4.75E-09	1.21E-08	2.58E-08	1.42E-08
1.05E-08	1.77E-08	2.32E-08	1.71E-08
1.55E-08	2.25E-08	1.83E-08	1.88E-08
2.06E-08	2.66E-08	1.32E-08	2.01E-08
2.39E-08	2.81E-08	6.78E-09	1.96E-08
2.66E-08	2.81E-08	5.36E-09	2.00E-08
2.79E-08	2.76E-08	1.09E-08	2.21E-08
2.83E-08	2.60E-08	1.66E-08	2.36E-08
2.77E-08	2.21E-08	2.13E-08	2.37E-08
2.59E-08	1.71E-08	2.52E-08	2.28E-08
2.33E-08	1.18E-08	2.71E-08	2.07E-08
1.92E-08	5.48E-09	2.83E-08	1.77E-08
			2.71E-08

Table B: B field transmitted through empty core rock

with empty CR_1	with empty CR_2	with empty CR_3	Average
2.46E-07	2.85E-07	2.37E-07	2.56E-07
9.79E-09	2.70E-08	1.89E-08	1.86E-08
1.83E-08	2.12E-08	1.49E-08	1.81E-08
2.52E-08	1.41E-08	8.80E-09	1.60E-08
2.75E-08	7.73E-09	3.48E-09	1.29E-08
2.75E-08	1.81E-08	8.39E-09	1.80E-08
2.44E-08	2.46E-08	1.33E-08	2.08E-08
1.74E-08	2.74E-08	1.86E-08	2.11E-08
9.12E-09	2.79E-08	2.24E-08	1.98E-08
1.31E-08	2.62E-08	2.63E-08	2.19E-08
2.11E-08	2.01E-08	2.79E-08	2.30E-08
2.63E-08	1.11E-08	2.81E-08	2.18E-08
2.73E-08	9.94E-09	2.81E-08	2.18E-08
2.72E-08	1.93E-08	2.74E-08	2.46E-08
2.33E-08	2.51E-08	2.49E-08	2.44E-08
1.53E-08	2.81E-08	2.27E-08	2.20E-08
5.87E-09	2.74E-08	1.83E-08	1.72E-08
1.60E-08	2.51E-08	1.29E-08	1.80E-08
2.35E-08	1.82E-08	7.43E-09	1.64E-08
2.70E-08	9.12E-09	4.75E-09	1.36E-08
2.77E-08	1.18E-08	1.05E-08	1.67E-08
2.58E-08	2.07E-08	1.55E-08	2.07E-08
2.06E-08	2.62E-08	2.06E-08	2.24E-08
1.18E-08	2.80E-08	2.39E-08	2.12E-08
9.97E-09	2.72E-08	2.66E-08	2.13E-08
1.97E-08	2.33E-08	2.79E-08	2.36E-08
2.56E-08	1.66E-08	2.83E-08	2.35E-08
2.76E-08	6.38E-09	2.77E-08	2.06E-08
2.76E-08	1.46E-08	2.59E-08	2.27E-08
2.50E-08	2.23E-08	2.33E-08	2.36E-08
1.77E-08	2.67E-08	1.92E-08	2.12E-08
			2.72E-08

Table C: B field transmitted through flooded core rock

with flooded CR_1	with flooded CR_2	with flooded CR_3	Average
2.61E-07	2.82E-07	2.79E-07	2.74E-07
2.32E-08	3.22E-08	4.56E-08	3.37E-08
3.94E-08	4.40E-08	4.47E-08	4.27E-08
4.50E-08	4.55E-08	3.57E-08	4.21E-08
4.51E-08	4.10E-08	2.05E-08	3.56E-08
3.44E-08	2.50E-08	3.88E-08	3.27E-08
2.33E-08	3.32E-08	4.56E-08	3.40E-08
3.92E-08	4.53E-08	4.50E-08	4.32E-08
4.54E-08	4.55E-08	3.65E-08	4.25E-08
4.46E-08	4.04E-08	1.96E-08	3.49E-08
3.36E-08	2.37E-08	3.71E-08	3.15E-08
2.35E-08	3.43E-08	4.50E-08	3.43E-08
4.04E-08	4.49E-08	4.53E-08	4.35E-08
4.52E-08	4.59E-08	3.75E-08	4.29E-08
4.39E-08	3.98E-08	2.12E-08	3.50E-08
3.34E-08	2.32E-08	3.62E-08	3.10E-08
2.45E-08	3.55E-08	4.53E-08	3.51E-08
4.07E-08	4.51E-08	4.54E-08	4.38E-08
4.55E-08	4.55E-08	3.95E-08	4.35E-08
4.44E-08	3.86E-08	2.26E-08	3.52E-08
3.32E-08	2.10E-08	3.49E-08	2.97E-08
2.45E-08	3.64E-08	4.48E-08	3.52E-08
4.09E-08	4.48E-08	4.53E-08	4.37E-08
4.50E-08	4.52E-08	4.04E-08	4.35E-08
4.42E-08	3.74E-08	2.37E-08	3.51E-08
3.20E-08	1.98E-08	3.34E-08	2.84E-08
2.45E-08	3.70E-08	4.44E-08	3.53E-08
4.12E-08	4.48E-08	4.51E-08	4.37E-08
4.53E-08	4.52E-08	4.07E-08	4.38E-08
4.41E-08	3.71E-08	2.50E-08	3.54E-08
3.22E-08	2.06E-08	3.20E-08	2.83E-08
			4.5E-08

Table D: B field transmitted after 2 hours

after 2 hrs_1	after 2 hrs_2	after 2 hrs_3	Average
4.50E-08	4.55E-08	4.56E-08	4.54E-08
4.51E-08	4.10E-08	4.47E-08	4.36E-08
3.44E-08	2.50E-08	3.57E-08	3.17E-08
2.33E-08	3.32E-08	2.05E-08	2.57E-08
3.92E-08	4.53E-08	3.88E-08	4.11E-08
4.54E-08	4.55E-08	4.56E-08	4.55E-08
4.46E-08	4.04E-08	4.50E-08	4.33E-08
3.36E-08	2.37E-08	3.65E-08	3.13E-08
2.35E-08	3.43E-08	1.96E-08	2.58E-08
4.04E-08	4.49E-08	3.71E-08	4.08E-08
4.52E-08	4.59E-08	4.50E-08	4.54E-08
4.39E-08	3.98E-08	4.53E-08	4.30E-08
3.34E-08	2.32E-08	3.75E-08	3.14E-08
2.45E-08	3.55E-08	2.12E-08	2.70E-08
4.07E-08	4.51E-08	3.62E-08	4.07E-08
4.55E-08	4.55E-08	4.53E-08	4.54E-08
4.44E-08	3.86E-08	4.54E-08	4.28E-08
3.32E-08	2.10E-08	3.95E-08	3.12E-08
2.45E-08	3.64E-08	2.26E-08	2.78E-08
4.09E-08	4.48E-08	3.49E-08	4.02E-08
4.50E-08	4.52E-08	4.48E-08	4.50E-08
4.42E-08	3.74E-08	4.53E-08	4.23E-08
3.20E-08	1.98E-08	4.04E-08	3.07E-08
2.45E-08	3.70E-08	2.37E-08	2.84E-08
4.12E-08	4.48E-08	3.34E-08	3.98E-08
4.53E-08	4.52E-08	4.44E-08	4.50E-08
4.41E-08	3.71E-08	4.51E-08	4.21E-08
3.22E-08	2.06E-08	4.07E-08	3.12E-08
2.54E-08	3.81E-08	2.50E-08	2.95E-08
4.14E-08	4.54E-08	3.20E-08	3.96E-08
4.55E-08	4.53E-08	4.48E-08	4.52E-08
			3.77E-08

Table E: B field transmitted after 4 hours

after 4 hrs_1	after 4 hrs_2	after 4 hrs_3	Average
4.50E-08	4.49E-08	4.49E-08	4.49E-08
3.88E-08	3.41E-08	3.41E-08	3.57E-08
4.18E-08	4.33E-08	4.33E-08	4.28E-08
4.57E-08	4.59E-08	4.59E-08	4.58E-08
3.83E-08	3.31E-08	3.31E-08	3.48E-08
4.11E-08	4.40E-08	4.40E-08	4.30E-08
4.56E-08	4.60E-08	4.60E-08	4.59E-08
3.82E-08	3.35E-08	3.35E-08	3.50E-08
4.22E-08	4.34E-08	4.34E-08	4.30E-08
4.53E-08	4.57E-08	4.57E-08	4.55E-08
3.74E-08	3.21E-08	3.21E-08	3.39E-08
4.22E-08	4.50E-08	4.50E-08	4.40E-08
4.49E-08	4.58E-08	4.58E-08	4.55E-08
3.66E-08	3.18E-08	3.18E-08	3.34E-08
4.21E-08	4.37E-08	4.37E-08	4.31E-08
4.52E-08	4.55E-08	4.55E-08	4.54E-08
3.70E-08	3.10E-08	3.10E-08	3.30E-08
4.23E-08	4.49E-08	4.49E-08	4.40E-08
4.53E-08	4.53E-08	4.53E-08	4.53E-08
3.69E-08	2.98E-08	2.98E-08	3.22E-08
4.32E-08	4.37E-08	4.37E-08	4.35E-08
4.48E-08	4.54E-08	4.54E-08	4.52E-08
3.67E-08	3.06E-08	3.06E-08	3.26E-08
4.23E-08	4.48E-08	4.48E-08	4.40E-08
4.52E-08	4.49E-08	4.49E-08	4.50E-08
3.66E-08	2.96E-08	2.96E-08	3.19E-08
4.30E-08	4.53E-08	4.53E-08	4.45E-08
4.53E-08	4.54E-08	4.54E-08	4.53E-08
3.64E-08	2.87E-08	2.87E-08	3.13E-08
4.27E-08	4.51E-08	4.51E-08	4.43E-08
4.56E-08	4.49E-08	4.49E-08	4.51E-08
			4.09E-08

Table F: B field transmitted after 10 hours

after 10 hrs_1	after 10 hrs_2	after 10 hrs_3	Average
4.57E-08	4.64E-08	4.58E-08	4.60E-08
4.53E-08	3.48E-08	4.24E-08	4.08E-08
3.34E-08	4.52E-08	4.16E-08	4.01E-08
4.62E-08	4.64E-08	4.61E-08	4.62E-08
4.33E-08	2.92E-08	3.74E-08	3.66E-08
3.97E-08	4.57E-08	4.39E-08	4.31E-08
4.67E-08	4.52E-08	4.60E-08	4.60E-08
4.02E-08	3.48E-08	3.08E-08	3.53E-08
4.27E-08	4.60E-08	4.54E-08	4.47E-08
4.62E-08	4.38E-08	4.56E-08	4.52E-08
3.38E-08	3.99E-08	3.22E-08	3.53E-08
4.52E-08	4.62E-08	4.61E-08	4.58E-08
4.62E-08	4.04E-08	4.49E-08	4.38E-08
2.99E-08	4.26E-08	3.74E-08	3.66E-08
4.60E-08	4.62E-08	4.55E-08	4.59E-08
4.44E-08	3.42E-08	4.24E-08	4.03E-08
3.69E-08	4.58E-08	4.07E-08	4.11E-08
4.57E-08	4.64E-08	4.64E-08	4.62E-08
4.28E-08	2.83E-08	3.74E-08	3.62E-08
4.21E-08	4.57E-08	4.38E-08	4.39E-08
4.60E-08	4.58E-08	4.58E-08	4.59E-08
3.81E-08	3.47E-08	3.17E-08	3.49E-08
4.37E-08	4.60E-08	4.61E-08	4.53E-08
4.63E-08	4.33E-08	4.64E-08	4.53E-08
3.10E-08	3.85E-08	2.99E-08	3.31E-08
4.62E-08	4.58E-08	4.62E-08	4.61E-08
4.56E-08	3.94E-08	4.57E-08	4.36E-08
3.23E-08	4.34E-08	3.46E-08	3.67E-08
4.56E-08	4.65E-08	4.66E-08	4.63E-08
4.36E-08	3.44E-08	4.25E-08	4.02E-08
3.88E-08	4.45E-08	4.02E-08	4.12E-08
			4.19E-08

Table G: B field transmitted after 12 hours

after 12 hrs_1	after 12 hrs_2	after 12 hrs_3	Average
4.41E-08	2.86E-08	4.45E-08	3.91E-08
4.36E-08	4.18E-08	4.04E-08	4.19E-08
3.43E-08	4.39E-08	2.63E-08	3.48E-08
2.50E-08	4.24E-08	3.40E-08	3.38E-08
4.05E-08	2.68E-08	4.37E-08	3.70E-08
4.43E-08	3.31E-08	4.41E-08	4.05E-08
4.35E-08	4.38E-08	3.90E-08	4.21E-08
2.93E-08	4.44E-08	2.34E-08	3.23E-08
3.21E-08	3.94E-08	3.68E-08	3.61E-08
4.32E-08	2.37E-08	4.41E-08	3.70E-08
4.43E-08	3.76E-08	4.44E-08	4.21E-08
3.92E-08	4.44E-08	3.64E-08	4.00E-08
2.43E-08	4.40E-08	2.41E-08	3.08E-08
3.62E-08	3.40E-08	3.86E-08	3.63E-08
4.37E-08	2.58E-08	4.48E-08	3.81E-08
4.44E-08	4.04E-08	4.42E-08	4.30E-08
3.54E-08	4.46E-08	3.32E-08	3.78E-08
2.57E-08	4.33E-08	2.71E-08	3.20E-08
3.99E-08	3.12E-08	4.11E-08	3.74E-08
4.48E-08	2.97E-08	4.46E-08	3.97E-08
4.28E-08	4.28E-08	4.26E-08	4.27E-08
3.06E-08	4.42E-08	3.02E-08	3.50E-08
3.02E-08	4.02E-08	3.07E-08	3.37E-08
4.29E-08	2.71E-08	4.22E-08	3.74E-08
4.42E-08	3.33E-08	4.45E-08	4.07E-08
3.97E-08	4.44E-08	4.14E-08	4.18E-08
2.48E-08	4.46E-08	2.64E-08	3.19E-08
3.58E-08	3.84E-08	3.33E-08	3.58E-08
4.41E-08	2.21E-08	4.38E-08	3.66E-08
4.47E-08	3.71E-08	4.45E-08	4.21E-08
3.67E-08	4.45E-08	3.94E-08	4.02E-08
			3.77E-08

Table H: B field transmitted after 18 hours

after 18 hrs_1	after 18 hrs_2	after 18 hrs_3	Average
3.68E-08	3.49E-08	4.02E-08	3.73E-08
2.70E-08	2.59E-08	4.02E-08	3.10E-08
2.89E-08	3.02E-08	3.55E-08	3.16E-08
3.71E-08	3.76E-08	2.62E-08	3.36E-08
4.02E-08	4.09E-08	3.03E-08	3.71E-08
3.95E-08	3.92E-08	3.78E-08	3.88E-08
3.43E-08	3.26E-08	4.04E-08	3.58E-08
2.49E-08	2.40E-08	3.98E-08	2.96E-08
3.11E-08	3.21E-08	3.26E-08	3.20E-08
3.89E-08	3.88E-08	2.45E-08	3.40E-08
4.04E-08	4.05E-08	3.28E-08	3.79E-08
3.91E-08	3.82E-08	4.00E-08	3.91E-08
3.10E-08	3.03E-08	4.00E-08	3.38E-08
2.46E-08	2.62E-08	3.81E-08	2.96E-08
3.41E-08	3.46E-08	2.95E-08	3.27E-08
4.05E-08	3.99E-08	2.63E-08	3.56E-08
4.07E-08	4.09E-08	3.51E-08	3.89E-08
3.76E-08	3.60E-08	4.07E-08	3.81E-08
2.81E-08	2.71E-08	4.03E-08	3.19E-08
2.73E-08	2.85E-08	3.65E-08	3.08E-08
3.65E-08	3.75E-08	2.68E-08	3.36E-08
4.04E-08	4.05E-08	2.85E-08	3.65E-08
4.04E-08	4.00E-08	3.70E-08	3.91E-08
3.52E-08	3.46E-08	4.02E-08	3.67E-08
2.57E-08	2.55E-08	3.99E-08	3.04E-08
3.01E-08	3.03E-08	3.45E-08	3.16E-08
3.78E-08	3.92E-08	2.47E-08	3.39E-08
4.09E-08	4.05E-08	3.10E-08	3.74E-08
4.02E-08	3.87E-08	3.85E-08	3.91E-08
3.28E-08	3.25E-08	4.03E-08	3.52E-08
2.39E-08	2.38E-08	3.89E-08	2.89E-08
			3.46E-08

Table I: B field transmitted after 24 hours

after 24 hrs_1	after 24 hrs_2	after 24 hrs_3	Average
3.13E-08	2.79E-08	3.07E-08	2.99E-08
3.63E-08	3.56E-08	3.61E-08	3.60E-08
3.61E-08	3.63E-08	3.69E-08	3.64E-08
3.24E-08	3.43E-08	3.26E-08	3.31E-08
2.82E-08	2.67E-08	2.73E-08	2.74E-08
3.56E-08	3.35E-08	3.44E-08	3.45E-08
3.62E-08	3.63E-08	3.61E-08	3.62E-08
3.46E-08	3.57E-08	3.49E-08	3.51E-08
2.76E-08	2.91E-08	2.81E-08	2.83E-08
3.24E-08	3.15E-08	3.21E-08	3.20E-08
3.69E-08	3.59E-08	3.65E-08	3.64E-08
3.54E-08	3.63E-08	3.64E-08	3.60E-08
3.00E-08	3.14E-08	3.13E-08	3.09E-08
3.00E-08	2.90E-08	2.97E-08	2.96E-08
3.59E-08	3.55E-08	3.58E-08	3.57E-08
3.66E-08	3.76E-08	3.62E-08	3.68E-08
3.33E-08	3.38E-08	3.37E-08	3.36E-08
2.72E-08	2.71E-08	2.70E-08	2.71E-08
3.50E-08	3.41E-08	3.40E-08	3.44E-08
3.61E-08	3.65E-08	3.64E-08	3.63E-08
3.50E-08	3.56E-08	3.63E-08	3.56E-08
2.91E-08	2.86E-08	2.94E-08	2.90E-08
3.18E-08	3.28E-08	3.10E-08	3.19E-08
3.65E-08	3.62E-08	3.57E-08	3.61E-08
3.61E-08	3.58E-08	3.65E-08	3.61E-08
3.22E-08	3.06E-08	3.28E-08	3.18E-08
2.85E-08	2.99E-08	2.84E-08	2.89E-08
3.51E-08	3.59E-08	3.51E-08	3.54E-08
3.62E-08	3.70E-08	3.62E-08	3.64E-08
3.45E-08	3.33E-08	3.51E-08	3.43E-08
2.76E-08	2.76E-08	2.83E-08	2.78E-08
			3.32E-08

Table J: B field transmitted after 36 hours

after 36 hrs_1	after 36 hrs_2	after 36 hrs_3	Average
3.59E-08	3.32E-08	3.59E-08	3.50E-08
3.27E-08	2.86E-08	3.28E-08	3.14E-08
2.96E-08	3.58E-08	3.03E-08	3.19E-08
3.54E-08	3.57E-08	3.59E-08	3.57E-08
3.54E-08	2.97E-08	3.54E-08	3.35E-08
2.85E-08	3.34E-08	2.84E-08	3.01E-08
3.38E-08	3.63E-08	3.36E-08	3.46E-08
3.55E-08	3.44E-08	3.54E-08	3.51E-08
3.30E-08	2.78E-08	3.37E-08	3.15E-08
2.95E-08	3.58E-08	2.94E-08	3.16E-08
3.59E-08	3.58E-08	3.62E-08	3.60E-08
3.59E-08	3.09E-08	3.62E-08	3.43E-08
2.94E-08	3.26E-08	3.03E-08	3.08E-08
3.33E-08	3.61E-08	3.26E-08	3.40E-08
3.60E-08	3.60E-08	3.65E-08	3.62E-08
3.42E-08	2.70E-08	3.37E-08	3.16E-08
2.88E-08	3.46E-08	2.82E-08	3.06E-08
3.54E-08	3.58E-08	3.52E-08	3.55E-08
3.58E-08	3.28E-08	3.55E-08	3.47E-08
2.94E-08	3.06E-08	3.09E-08	3.03E-08
3.33E-08	3.61E-08	3.21E-08	3.38E-08
3.57E-08	3.58E-08	3.62E-08	3.59E-08
3.41E-08	2.88E-08	3.47E-08	3.25E-08
2.90E-08	3.44E-08	2.70E-08	3.01E-08
3.58E-08	3.59E-08	3.50E-08	3.55E-08
3.59E-08	3.32E-08	3.59E-08	3.50E-08
3.02E-08	2.91E-08	3.20E-08	3.04E-08
3.29E-08	3.52E-08	3.19E-08	3.33E-08
3.58E-08	3.54E-08	3.60E-08	3.57E-08
3.41E-08	2.97E-08	3.59E-08	3.32E-08
2.82E-08	3.24E-08	2.69E-08	2.91E-08
			3.32E-08